

PEOPLE'S DEMOCRATIC REPUBLIC OF ALGERIA

MINISTRY OF HIGHER EDUCATION AND SCIENTIFIC RESEARCH

UNIVERSITY OF KASDI MERBAH OUARGLA

Faculty of Applied Sciences

Department of Process Engineering

Final year dissertation

ACADEMIC MASTER

FIELD: SCIENCE AND TECHNOLOGY

BRANCH: Petrochemical industries

SPECIALIZATION: Petroleum Refining Engineering

Presented By:

Hani Souheyb

Kouani Imane

TITLE:

**Simulation Study of CuO, Cu₂O and ZnO for Energy
Security Applications**

Publicly supported the: 01/06/2025

In front of a jury composed of:

Pr. FATHI Achi	(Univ. Ouargla)	President
Dr. ROUANE Azzeddine	(Univ. Ouargla)	Examiner
Dr. BACHA Oussama	(Univ. Ouargla)	Supervisor

Academic Year: 2024/2025

Dedication

To those whose prayers were the secret of my success and whose contentment
being the secret of my peace of mind.

To my beloved father, who instilled in my heart the meaning of determination
and was always my support and guide.

To my dear mother, the source of tenderness and my constant companion in
prayer,

To both of you I bow in gratitude, for you are the light that illuminates my path.

To my dear brothers, who have shared the details of my journey with me, with a
laugh, an advice, or a word of encouragement,

You have always been the pillar to which I return with confidence.

To my faithful friends, who shared my moments of fatigue and joy,

Those whose presence provided energy, whose patience provided support, and
whose questions provided motivation...to you all, from the bottom of my heart, my
sincere thanks.

And to my esteemed supervisor,

Thank you for your kind guidance, sincere concern, and patience that gave me
the confidence to complete this journey.

This thesis is the fruit of your support and guidance.

To all of you, I dedicate this note in gratitude, love, and appreciation beyond
words.

Hani Souheyb

Dedication

I WOULD LIKE TO DEDICATE MY THESIS
TO MY LOVING PARENTS
WHOSE CONTINUOUS EFFORTS, SUPPORT AND ENCOURAGEMENT
MADE IT POSSIBLE FOR ME TO DO THIS WORK.

Kouani Imane

Acknowledgement

All praise is due to God, by whose grace good deeds are accomplished and by whose favour all matters are made easy. May peace and blessings be upon the best of His creation, Muhammad ibn Abdullah, and upon all his family and companions.

We would like to express our heartfelt gratitude to all those who supported us throughout our academic journey, particularly in the preparation of this modest work.

We would also like to express our deepest gratitude to our supervisor, **Dr. BACHA Oussama**, for his wise guidance, valuable feedback and unwavering commitment to ensuring the quality of this work.

Our thanks also go to the committee, comprising **Pr. FATHI Achi, and Dr. ROUANE Azzeddine**, for agreeing to review this work and for their constructive comments on how to improve it.

Abstract

In the context of the growing global importance of solar photovoltaics as a vital source of renewable energy, the pursuit of more efficient and sustainable solar cells is of paramount importance. This study focused on exploring the potential of hybrid solar cell structures combining copper oxides (CuO and Cu₂O), known for their abundance and promising optical properties, and zinc oxide (ZnO), a commonly used material in solar cells. Using the powerful SCAPS-1D simulation software, the performance of these structures has been carefully analyzed, focusing on determining the effect of key parameters, such as layer dimensions and material concentrations, on the power conversion efficiency. This research aims to evaluate the extent to which these configurations can contribute to improving the future of solar energy and meeting the growing global demand for clean energy.

Keywords: Solar cell, CuO, Cu₂O and ZnO absorber layers, thin films, simulation SCAPS-1D.

Résumé

Dans le contexte de l'importance croissante de l'énergie solaire photovoltaïque comme source d'énergie renouvelable vitale à l'échelle mondiale, la recherche de cellules solaires plus efficaces et durables est primordiale. Cette étude s'est concentrée sur l'exploration du potentiel des structures de cellules solaires hybrides combinant des oxydes de cuivre (CuO et Cu₂O), qui sont abondants et présentent des propriétés optiques intéressantes, et de l'oxyde de zinc (ZnO), un matériau couramment utilisé dans les cellules solaires. Grâce au puissant logiciel de simulation SCAPS-1D, les performances de ces structures ont été analysées en profondeur, en se concentrant sur l'effet de paramètres clés tels que les dimensions des couches et les concentrations de matériaux sur le rendement de conversion d'énergie. Cette recherche vise à évaluer dans quelle mesure ces configurations peuvent contribuer à assurer l'avenir de l'énergie solaire et à répondre à la demande croissante en énergie propre à l'échelle mondiale.

Mots clés : cellule solaire, couches absorbantes CuO, Cu₂O et ZnO, films minces, simulation.

ملخص

في سياق الأهمية العالمية المتزايدة للطاقة الشمسية الكهروضوئية كمصدر حيوي للطاقة المتجددة، يكتسب السعي لتطوير خلايا شمسية أكثر كفاءة واستدامة. ركزت هذه الدراسة على استكشاف إمكانات هياكل الخلايا الشمسية التي تجمع بين أكاسيد النحاس، المعروفة بوفرتها وخصائصها البصرية الواعدة، أكسيد الزنك وهو مادة شائعة الاستخدام في الخلايا الشمسية. باستخدام برنامج المحاكاة القوي، تم تحليل أداء هذه الهياكل بعناية، مع التركيز على تحديد تأثير المعايير الرئيسية، مثل SCAPS-1D أبعاد الطبقة، وتركيزات المواد، على كفاءة تحويل الطاقة. يهدف هذا البحث إلى تقييم مدى مساهمة هذه التكوينات في تحين مستقبل الطاقة الشمسية وتلبية الطلب العالمي المتزايد على الطاقة النظيفة.

الكلمات المفتاحية: الخلايا الشمسية، أكسيد النحاس، ثنائي أكسيد النحاس، أكسيد الزنك، الأغشية الرقيقة، برنامج المحاكاة SCAPS-1D

List of Tables

Chapter I: Physical properties of CuO, Cu₂O and ZnO materials

Table I.1: Physical Properties of CuO	3
Table I.2: Physical properties of Cu ₂ O	6
Table I.3: Physical Properties of ZnO	8

Chapter III: Results and discussions

Table III.1: Parameters values of CuO and ZnO solar cell structures used in SCAPS-1D	33
Table III.2: Parameters values of Cu ₂ O and ZnO solar cell structures used in SCAPS-1D	38
Table III.3: Properties of Materials used in our simulation.	43
Table III.4: Summary of the Properties of the Materials included in the numerical simulation wok.	44
Table III.5 : Table showing someone's CuO/ZnO simulation results and our results.	44
Table III.6 : Table showing someone's Cu ₂ O/ZnO simulation results and our results	45
Table III.7: Summary of the Properties of the Materials included in the numerical simulation wok	45
Table III.8: Table showing someone's Cu ₂ O/ZnO simulation results and our results.	46

List of Figures

Chapter I: Physical properties of CuO and Cu₂O materials

Figure I.1: Unit cell structure of copper (CuO) oxide	2
Figure I.2: Unit cell structure of cuprous (Cu ₂ O) oxide	5
Figure I.3: Unit cell structure of Zinc oxide-ZnO	7
Figure I.4: CuO structure as crystallizes	10
Figure I.5: Illustrates the cubic structure of Cu ₂ O	13
Figure I.6: Unit cell structure of Zinc oxide	15
Figure I.7: MD-calculated constant-volume heat capacity of the ZnO with RS-type and ZB-type cubic structures, respectively	17

Chapter II: Presentation of SCAPS-1D simulator

Figure II.1: Main Software User Interface.	21
Figure II.2: Problem Definition Icon.	22
Figure II.3: File Uploading Feature Icon.	23
Figure II.4: Device Operating Point Display.	24
Figure II.5: Illumination Settings Section.	24
Figure II.6: Simulation Measurement Type Options.	25
Figure II.7: Single-Shot Calculation Button.	25
Figure II.8: Simulation Current Stage Display.	26
Figure II.9: Power Range Curve Panel.	27
Figure II.10: Data Output Control Options.	27
Figure II.11: Left Device Contact Window.	28
Figure II.12: The interface between the layers.	29
Figure II.13: Defect Settings Interface Panel.	29

Chapter III: Results and discussions

Figure III.1: Unit cell structure of copper (CuO) oxide	32
Figure III.2: Band diagram for CuO solar cells structures used in the simulation	34
Figure III.3: CuO absorber thickness	35
Figure III.4: Quantum efficiency versus wavelength of CuO solar cell structures	36
Figure III.5: Acceptor concentration of absorber layer NA(CuO) on cell performances	37
Figure III.6: Band diagram for Cu ₂ O solar cells structures used in the Simulation	39
Figure III.7: Cu ₂ O absorber thickness	40
Figure III.8: Quantum efficiency versus wavelength of Cu ₂ O solar cell structures	41
Figure III.9: Acceptor concentration of absorber layer NA(Cu ₂ O) on cell performance	42

TABLE OF CONTENTS

Dedication

Acknowledgement

Abstract

List of Tables

List of Figures

General Introduction..... I

Chapter I: Physical properties of CuO, Cu₂O and ZnO materials

I.1. Introduction..... 1

I.2. Basics of material science 1

I.2.1. Presentation of CuO, Cu₂O and ZnO compounds 1

I.2.1.1. Properties of copper oxide (CuO) 1

I.2.1.2. Applications of copper oxide (CuO) 4

I.2.1.3. Properties of copper oxide (Cu₂O) 4

I.2.1.4. Applications of copper oxide (Cu₂O) 6

I.2.1.5. Properties of zinc oxide-ZnO 7

I.2.1.6. Applications of zinc oxid (ZnO) 8

I.3. Semiconduction layers 8

I.3.1. Intrinsic semiconductors 9

I.3.2. Extrinsic semiconductor 9

I.4. In-depth analysis of CuO material..... 10

I.4.1. Structure and stability of CuO material 10

I.4.2. Electronic and optical properties of CuO material 11

I.4.3. Mechanical and thermal properties of CuO material 12

I.5. In-depth analysis of Cu₂O material 13

I.5.1. Structure and stability of Cu₂O material 13

I.5.2. Electronic and optical properties of Cu ₂ O material	13
I.5.3. Mechanical and thermal properties of Cu ₂ O material	14
I.6. In-depth analysis of ZnO material.....	14
I.6.1. Structure and stability of ZnO material	14
I.6.2. Electronic and optical properties of ZnO material.....	16
I.6.3. Mechanical and thermal properties of ZnO material.....	16
I.7. Applications of CuO/ZnO heterojunction.....	18
I.8. Applications of Cu₂O /ZnO heterojunction.....	18
I.9. Conclusion.....	19

Chapter II: Presentation of SCAPS-1D simulator

II.1. Introduction.....	21
II.2. The basics	21
II.2.1. To start SCAPS.....	22
II.2.2. Define the problem	22
II 2.3. Define the working point	23
II 2.4. Select the measurement(s) to simulate.....	24
II 2.5. Start the calculation(s).....	25
II 2.6. Display the simulated curves	26
II 2.6.1. Control panel data output options in SCAPS.....	27
II.3. Left contact	28
II.4. Right contact.....	29
II.5. Interface between layers.....	29
II.6. Conclusion	30

Chapter III: Results and discussions

III.1. Introduction	32
III.2. Modeling a copper oxide (CuO) and zinc oxide (ZnO) solar cell substrate	32
defined.	
III.3. Physical model and simulation parameters	32

III.4. Band diagram	33
III.5. Thickness optimization of CuO absorber layer	35
III.6. Quantum efficiency QE	35
III.7. Optimization of acceptor density NA(CuO)	36
III.8. Modeling a copper oxide (Cu₂O) and zinc oxide (ZnO) solar cell substrate.....	37
not defined.	
III.9. Physical model and simulation parameter	38
III.10. Band diagram	38
III.11. Thickness optimization of Cu₂O absorber layer	39
III.12. Quantum efficiency QE	41
III.13. Optimization of acceptor density NA (Cu₂O).....	41
III.14. Analysis of results.....	42
III.14.1. Thickness of CuO and Cu ₂ O	42
III.14.2. Acceptor density NA (CuO), NA (Cu ₂ O).....	42
III.15. Solar cell performance comparison	43
III.16. Conclusion.....	46
General conclusion.....	49
References.....	50

General Introduction

The current global energy crisis, which encompasses economic, environmental and social dimensions, requires a fundamental shift in our transition to renewable energy sources. Our ecological footprint has exceeded the planet's biocapacity since the since the 1980s[1], highlighting the unsustainability of our current development model. An energy economy based on fossil fuels is unsustainable due to resource depletion, climate change risks from greenhouse gas emissions, and the need for energy security[2].

At the same time, energy demand is escalating, especially in developing where more than a billion people lack access to electricity. As a result, renewable energy sources such as hydropower, biomass, wind and solar power are poised for significant expansion. Given the high demand, intermittent nature and varying storage capabilities of each energy source, a complementary development of different renewable of different renewable energy sources is essential. Solar energy occupies a unique position in this landscape. The sun provides more energy in a single hour than humanity consumes in a year. Moreover, indirectly supports almost all other energy sources, except nuclear and geothermal energy, through processes such as photosynthesis, the water cycle, and air convection. Within the solar sector, photovoltaic (PV) energy is distinguished from thermodynamic solar energy in that it generates electricity directly, eliminating the need for for steam cycles or rotating mechanical components. Most importantly, it doesn't require direct sunlight, making it an excellent choice for temperate regions, which are often characterized by diffuse diffuse sunlight due to cloud cover. Photovoltaics have immense potential. For example, in France, covering 5000 km² with 10% efficient solar panels could produce the equivalent of 550 TWh. equivalent of 550 TWh, equivalent to current electricity production [3]. In addition, PV is a decentralized energy solution that is already cost-competitive for remote locations (such as the Algerian Sahara). Sahara) where grid connection is prohibitively expensive. To accelerate adoption, it is critical to optimize costs, including the end consumer price and the price, as well as the raw materials and energy used to produce efficient PV modules. The basic principle of a classic PV cell is a junction of two semiconductors that semiconductors that generate an electric current when exposed to light - the photovoltaic effect. A PV module consists of interconnected PV cells that form the basic unit for solar installations. Several generations of PV technologies have been developed. The first generation, based on silicon cells, achieved maximum laboratory efficiencies of 20% for polycrystalline silicon and 25% for monocrystalline silicon[3]. Industrial efficiencies of 15 to 20%, and silicon-based cells

still dominate the market (85% in market (85% in 2010). However, the numerous manufacturing steps and high contribute to their relatively high cost.

The second generation focuses on thin-film cells, which are characterized by significant and require about 100 times less material (a few μm thick) than silicon cells compared to silicon cells (about 0.2 mm thick). These offer several advantages, including deposition on flexible substrates (expanding application possibilities) Simple, fast, multi-step processes at moderate temperatures. As a result, energy payback time for thin-film modules is about one year, compared to about two years for approximately two years for silicon cells. Thin-film technologies are gaining market share market share (14% worldwide in 2010, or 2.8 GW).

Industrially, thin-film sectors are generally categorized by the materials used. Hydrogenated amorphous silicon (a-Si:H) thin films are an established industry. industry that produces large area flexible solar panels. However, stabilized module efficiencies remain around 8%, with laboratory tandem cell efficiencies reaching as high as 13% with microcrystalline silicon. Industrial module efficiencies range from 15 to 20%, and silicon-based cells still dominate the market (85% in market (85% in 2010)[4]. However, the numerous manufacturing steps and high temperatures required The second generation focuses on thin-film cells, which are characterized by significant absorption power and require about 100 times less material (a few absorption power) and require about 100 times less material (a few μm thick) compared to silicon compared to silicon cells (about 0.2 mm thick). These offer several advantages, including deposition on flexible substrates (expanding application possibilities) Simple, fast, multi-step processes at moderate temperatures. As a result energy payback time for thin-film modules is about one year, compared to about two years for approximately two years for silicon cells. Thin-film technologies are gaining market share market share (14% worldwide in 2010, representing 2.8 GW).

This work investigates the photovoltaic parameters of thin film solar cells based on based on CuO and Cu₂O . In particular, the CuO/ZnO and Cu₂O /ZnO heterojunction structures, where p- type CuO or Cu₂O thin films serve as the absorber. layers, the region where electron-hole pairs are generated upon illumination. A PN junction is formed between the p-type CuO or Cu₂O absorber layer and the n-type ZnO which acts as the window layer. Solar cell simulation is performed using a powerful one-dimensional tool called SCAPS-1D simulator.

The study calculates and analyzes photovoltaic parameters such as short-circuit current

density (JSC), open- circuit voltage (VOC), fill factor voltage (VOC), fill factor (FF), and conversion efficiency (η). These parameters are derived directly or indirectly from the current-voltage characteristic (J-V) and the quantum efficiency (QE). The study also examines the effects of variations in the physical and geometrical properties of the structure, including the including the thickness of the CuO and Cu₂O layers and the doping concentrations in the regions that interface with the CuO and Cu₂O absorbers.

The thesis is divided into three chapters. The first chapter studies the physical properties of metal oxides (CuO, Cu₂O and ZnO). The second chapter presents the SCAPPS simulator mechanism and explains how to conduct simulations using it. The third chapter summaries and presents the obtained results.

Chapter I

Physical properties of CuO, Cu₂O and ZnO materials

I.1. Introduction

Copper oxides (Cu₂O, CuO) have two different crystal structures, colors, and physical properties. Both are good candidates for photovoltaic applications because they are inexpensive, non-toxic, and have high electrical and optical properties. They are both p-type semiconductors with band gaps of 2.1 and 1.2-1.75 eV, respectively, which makes them good at absorbing light and can be used in solar cells. Researchers have studied how the combination of CuO with other materials, such as SnO₂, Si, and Cu₂O, can improve the performance of solar cells[5].

Among the most extensively studied p-type semiconductors are CuO and Cu₂O, while ZnO is an established n-type semiconductor. The combination of CuO, Cu₂O, and ZnO in various heterojunction structures has demonstrated enhanced performance in solar cells, photocatalysis, and sensing applications due to their synergistic electronic and chemical properties.

This chapter provides a comprehensive analysis of the physical properties of these materials, exploring their structural, electronic, optical, mechanical, and thermal properties.

I.2. Basics of material science

I.2.1. Presentation of CuO, Cu₂O and ZnO compounds

I.2.1.1. Properties of copper oxide (CuO)

CuO, known in its natural state as tenorite, is a type of copper oxide used as a semiconducting material. Copper, known as Cu, has an atomic number of 29 (see Figure I.1) and is a vital component necessary for the survival of both flora and fauna, playing a critical role in the function of over 30 enzymes. It occurs naturally in various environmental media, including rocks, soil, water, and air.

Copper Oxide CuO has a number of positive and beneficial properties that have been explored in various research studies, including Electronics and Energy Storage. Due to its semiconducting nature, CuO is used in photovoltaic cells, batteries, and gas sensors. Its p-type conductivity enables the formation of heterojunctions with n-type materials, such as zinc oxide (ZnO). In energy storage, its high theoretical capacity and stability make copper oxide a promising material for lithium-ion batteries. These properties also make copper oxide a versatile material for use in next-generation electronics and power systems.

The structure of CuO directly influences its semiconducting, magnetic and catalytic properties, making it a versatile material for applications in electronics, energy and environmental technologies.

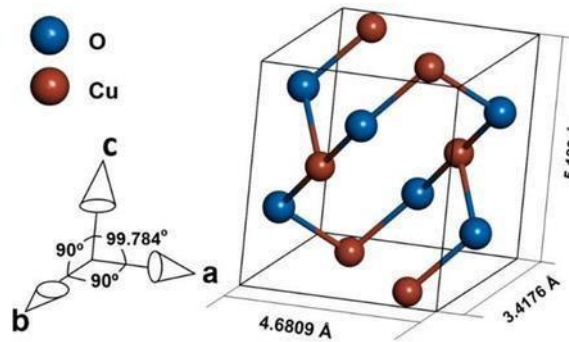


Figure I.1: Unit cell structure of copper (CuO) oxide[6].

The Figure I.1 effectively visualizes the monoclinic crystal structure of CuO, illustrating its lattice parameters, atomic connectivity, and bonding angles. This structure plays a critical role in CuO has electronic, optical, and magnetic properties, making it useful in semiconductors, batteries, and catalysis.

A. Physical properties

Copper oxide (CuO) is a black or dark brown solid with a monoclinic crystal structure. It is insoluble in water, but dissolves in acids to form copper salts.

CuO is a p-type semiconductor with a narrow band gap of about 1.2 eV, making it useful in electronic and photovoltaic applications. It has good thermal and electrical conductivity and is known for its stability under normal environmental conditions. It also has strong antimicrobial properties, making it valuable in medical applications, coatings and textiles. In addition, copper oxide plays an important role as a catalyst in various chemical reactions, including oxidation and reduction processes, and in environmental applications such as pollutant degradation and water purification. Its high surface reactivity and ability to facilitate electron transfer make it a key material in gas sensors, fuel cells and supercapacitors. In addition, due to its nanostructured forms, CuO has attracted considerable interest in nanotechnology, where it is used for energy storage, drug delivery and advanced coatings. These diverse applications highlight the importance of CuO has unique structural and electronic properties in both industrial and scientific advancements.

Its excellent optical absorption properties also make it a promising candidate for use in photodetectors and solar energy conversion. The following table lists some of the physical properties of CuO

Table I.1: Physical Properties of CuO[7][8].

Chemical Formula	CuO
Band Gap	1.2 eV
Molar Mass	79.545 g/mol
Density	6.315 g/cm ³
Appearance	black to brown powder.
Melting Point	1326°C (2419°F, 1599K).
Boiling Point	2000°C (3630°F, 2270K).
Solubility	Insoluble in water, alcohol and ammonium carbonate
Solubility	soluble in ammonium chloride and potassium cyanide
Crystal structure	Monoclinic
CuO	Copper(II) Oxide

Table I.1 lists the main physical properties of copper(II) oxide (CuO), highlighting its fundamental characteristics. CuO is a black to brown powder with a monoclinic crystal structure and a molar mass of 79.545 g/mol. It has a density of 6.315 g/cm³ and a relatively high melting point of 1326°C, which makes it thermally stable. Its boiling point reaches 2000°C, which enhances its stability under extreme conditions. CuO is insoluble in water, alcohol and ammonium carbonate, but soluble in ammonium chloride and potassium cyanide. With a narrow band gap of 1.2 eV, CuO exhibits semiconducting behavior, making it valuable for various electronic and catalytic applications.

B. Chemical Properties

Reaction of copper oxide (CuO) with hydrogen

Copper oxide gets converted to metallic copper along with the formation of water if allowed to react with hydrogen at high temperatures. This reaction is a classic example of a redox (Reduction + Oxidation) reaction.



This chemical reaction takes place at 200°C, first reducing copper to Cu, then oxidizing it by adding an oxygen atom to the hydrogen molecule.

Reaction of copper oxide with HCl

The equation below illustrates the interaction between cupric oxide (CuO) and hydrochloric acid (HCl):



In this reaction, cupric oxide and hydrochloric acid combine to form cupric chloride and water. The oxide acts as an oxygen acceptor, while the acid acts as a proton donor.

I.2.1.2. Applications of copper oxide (CuO)

Because many applications and their components are accessible in nature, they are inexpensive and have excellent thermal stability and electrochemical properties. The composite nature of copper oxide thin films has enabled them to demonstrate high efficiency in various applications, including

- High temperature superconductors
- solar panels
- Gas detection sensors
- Magnetic storage systems
- Varistors
- catalysts
- Antimicrobial functions
- photoelectrochemical cells
- Lithium batteries.

I.2.1.3. Properties of copper oxide (Cu₂O)

Cu₂O is an inorganic material with the chemical formula Cu₂O. It exhibits covalent properties like the mineral known as cuprite and was the first known oxide semiconductor [9].

Cu₂O (cuprous oxide) has a cubic crystal structure belonging to the simple cubic (SC) system. In this structure, copper (Cu⁺) ions are arranged in a face-centered cubic (FCC) sublattice, while oxygen (O²⁻) ions occupy the tetrahedral interstitials. Each oxygen ion is surrounded by four copper ions, and each copper ion is linearly coordinated by two oxygen ions (see Figure I.2). This

unique arrangement gives Cu₂O its distinctive electrical and optical properties, including a direct band gap of about 2.0 eV, making it useful in semiconductor and photovoltaic applications.

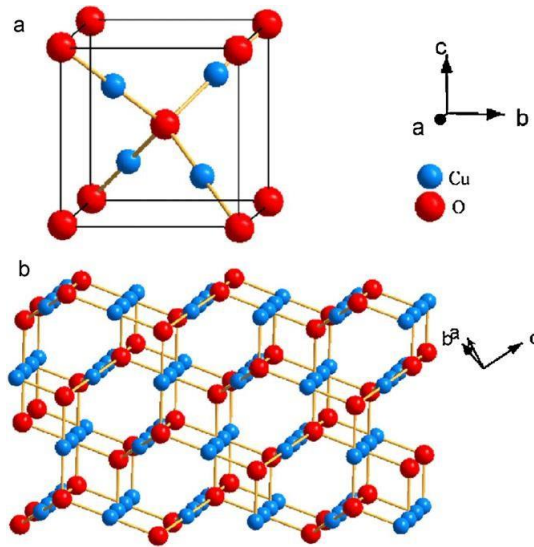


Figure I.2: Unit cell structure of cuprous (Cu₂O) oxide[10].

The cubic crystal structure of Cu₂O plays a crucial role in determining its electrical, optical and chemical properties. Its stability, together with its environmentally friendly and abundant nature, further enhances its applicability in various technological and industrial fields.

A. Physical properties

Cuprous oxide (Cu₂O) is a red inorganic compound with distinct physical properties that make it useful in various applications (see Table I.2).

Cuprous oxide (Cu₂O) is an important inorganic compound with unique physical and chemical properties that make it suitable for a wide range of industrial, scientific, and technological applications. As a p-type semiconductor with a direct band gap of 2.0 eV, it is widely studied for its potential in photovoltaics, photocatalysis, and optoelectronic devices. Its distinct red appearance and cubic crystal structure contribute to its use as a pigment in ceramics, glass, and coatings. Cu₂O has a high melting point of 1,232°C and a boiling point of 1,800°C, making it thermally stable under various conditions. With a molar mass of 143.09 g/mol and a density of 6 g/cm³, it is a relatively dense material with limited solubility, being insoluble in water. These properties not only define the fundamental properties of cuprous oxide, but also influence its functionality in various scientific and industrial fields. The physical properties of cuprous oxide (Cu₂O) play a crucial role in its diverse applications across multiple fields, ranging from energy conversion to protective coatings and electronic devices.

The table below provides a comprehensive overview of the most important physical properties of Cu₂O.

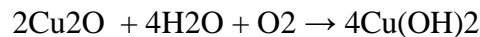
Table I.2: Physical properties of Cu₂O [10].

Cu₂O	Copper(I) Oxide.
Band Gap	2.0 eV
Molar Mass	143.09 g/mol
Density	6 g/cm ³
Melting Point	1,232 °C
Boiling Point	1,800 °C
Solubility	Insoluble in water
Appearance	Red
Crystal Structure	Cubic
Chemical Formula	Cu ₂ O

Copper oxide (Cu₂O) has unique properties that make it a promising material in many fields, making it an important compound in advanced materials research and development.

B. Chemical properties

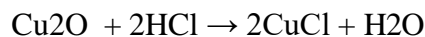
- ❖ Copper oxide (Cu₂O) reacts with water in the presence of oxygen to form copper hydroxide. This process can be described by the chemical equation:



- ❖ Copper oxide (Cu₂O) engages in a chemical reaction with hydrogen chloride

(HCl) to create copper chloride (CuCl) along with water.

- ❖ Below is the illustration of the process in which copper oxide and hydrogen chloride interact to produce copper chloride:



I.2.1.4. Applications of copper oxide (Cu₂O)

- ❖ It is used in antifouling coatings for the hulls of vessels. These coatings help stop the
- ❖ buildup of rust and other things that can damage a vessel's hull.
- ❖ It is also used in coatings for ceramics and glass.
- ❖ It is also used as a p-type semiconductor, which means it can conduct electricity. In the past, it was used to make photocells for light measurement

devices and rectifiers.

- ❖ Used as a fungicide and seed dressing [7].

I.2.1.5. Properties of zinc oxide-ZnO

Zinc oxide, also known as ZnO, is a type of mineral called zincite that occurs naturally; it can also be found in solid form as a colorless powder that ranges from off-white to light yellow, which exists in different forms: massive, thin layer, nanostructure. It has very interesting physicochemical properties (semiconductor, transparent in a wide range of the visible spectrum, good catalyst, non-toxic and abundant on Earth) (see Figure I.3)

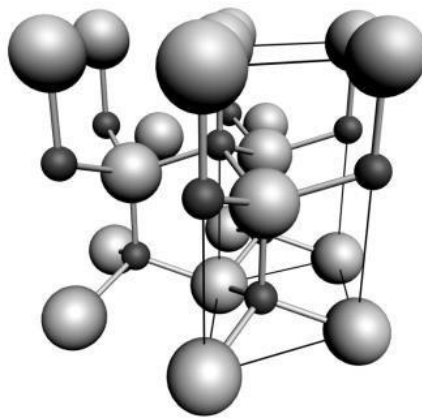


Figure I.3: The hexagonal wurtzite structure of ZnO. O atoms are shown as large white spheres, Zn atoms as smaller black spheres. One unit cell is outlined for clarity [11].

Zinc oxide (ZnO) has a hexagonal wurtzite crystal structure, which is the most thermodynamically stable form under ambient conditions. On the other hand, zinc oxide doesn't dissolve in water, but it does dissolve in acidic solutions [12].

A. Physical properties of zinc oxide-ZnO

Zinc oxide (ZnO) is a versatile material with exceptional physical properties that make it valuable in various industrial and technological applications.

The physical properties of ZnO, including its density, molar mass, and crystal structure, highlight its importance as a multifunctional material. The combination of these properties ensures that ZnO remains a key material for scientific research and industrial advancement.

Zinc oxide (ZnO) is a highly stable, thermally resistant, and chemically inert material with a wurtzite crystal structure. Due to its wide band gap (~3.37 eV), high thermal conductivity and UV absorption properties, it is widely used in electronics and medical applications. Its low solubility in water makes it suitable for long-term applications in coatings and protective films. Zinc oxide

(ZnO) is a widely used material due to its unique physical properties. The following table (Table I.3) summarizes the main physical properties of ZnO.

Table I.3: Physical Properties of ZnO [13].

Molecular formula	ZnO
Molar mass	81.408 g/mol
Appearance	White solid
Density	5.606 g / cm ³
Melting point	1975 °C
Boiling point	2360 °C
Structure	hexagonal wurtzite type
ZnO	Zinc oxide
Solubility in water	Soluble at 0.16 mg/100 mL (30 °C)

B. Chemical properties of zinc oxide-ZnO

The way zinc oxide is produced and changes in its crystal structure affect its activity. There are three temperature ranges that correspond to different chemical behaviors.

At temperatures above 1000°C, imperfections in the crystal structure can move from the surface to the core of the crystal. This allows different chemical reactions to reach their thermodynamic equilibrium.

Between 600°C and 1000°C, the defects remain on the surface, and only the surface reactions can occur in an easily reversible manner.

At temperatures below 600°C, the chemical reactivity of zinc oxide ceases. Zinc oxide can dissolve in many mineral acids and also reacts with bases to form zincate ions (Zn(OH)₄). However, it doesn't dissolve in liquid ammonia or liquid sulfur dioxide [12].

I.2.1.6. Applications of zinc oxid (ZnO)

- ❖ Semiconductors
- ❖ Transparent Conductive Films
- ❖ Piezoelectric Devices
- ❖ Gas Sensors

I.3. Semiconduction layers

Semiconductor substances contain two types of charge carriers: conduction electrons and holes. In a pure semiconductor substance, conduction electrons are generated when the material receives sufficient thermal energy, enabling the valence electrons from the valence band to gain enough

energy to jump to the conduction band and become conduction electrons. When these valence electrons make the transition to the conduction band, they generate holes within the valence band. These vacancies are referred to as holes. In this intrinsic, unaltered material, the total number of holes in the valence band matches the total number of conduction electrons present in the conduction band. A semiconductor material becomes an effective electronic component by manipulating its conductivity. However, in their natural state, semiconductor materials have poor conductivity for current. This is due to the limited existence of conduction electrons and holes within them. Nonetheless, a method called doping can enhance the conductivity of a semiconductor. Doping increases the number of charge carriers by introducing impurities that either provide additional conduction electrons or create more holes in the pure semiconductor material [14].

I.3.1. Intrinsic semiconductors

A semiconductor in its purest form is classified as an intrinsic semiconductor. The characteristics of this pure semiconductor include the following:

- ❖ Electrons and holes are generated only by thermal excitation.
- ❖ The number of free electrons is equal to the number of holes.
- ❖ The conductivity is low at room temperature.

I.3.2. Extrinsic semiconductor

A semiconductor that has been contaminated by the addition of impurities to a pure semiconductor is called an extrinsic semiconductor. There are two categories of extrinsic semiconductor, which are determined by the type of impurities incorporated. These categories are N-type extrinsic semiconductor and P-type extrinsic semiconductor.

A.N-Type extrinsic semiconductor

A small amount of pentavalent impurity is introduced into a clean semiconductor to form an extrinsic N-type semiconductor. This impurity has five valence electrons.

The free electrons generated produce an electric current. Consequently, when the impurity is incorporated into the clean semiconductor, it donates electrons for conduction.

- ❖ In N-type extrinsic semiconductors, conduction takes place primarily through electrons, which act as the main carriers, while the holes represent the lesser carriers.
- ❖ Since there is no increase in positive or negative charge, the electrons remain electrically neutral.

- ❖ When an electric field is introduced to a N-type semiconductor that includes a pentavalent impurity, the free electrons move toward the positive terminal. This behavior is referred to as N-type or negative conductivity.

B.P-Type extrinsic semiconductor

A small amount of trivalent impurity is added to a pure semiconductor to result in P-type extrinsic semiconductor. The added impurity has 3 valence electrons. For example, if Boron atom is added to the germanium atom, three of the valence electrons get attached with the Ge atoms, to form three covalent bonds. However, an additional electron in germanium doesn't create a bond. Since boron lacks an electron needed to establish a covalent bond, the resulting gap is regarded as a hole.

I.4. In-depth analysis of CuO material

Copper oxide (CuO), also known as cuprous oxide, is a substance of great importance due to its major involvement in several industrial processes, especially in catalysis and the production of superconducting materials. A detailed study of its structure and stability follows.

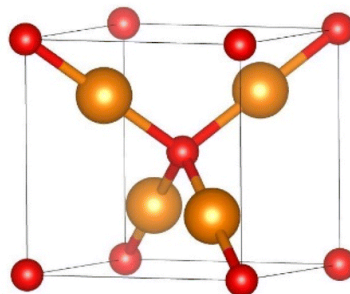
I.4.1. Structure and stability of CuO material

A. Structure properties

The arrangement of copper oxide (CuO) consists of each copper atom bonded to four oxygen atoms, forming a square planar shape[15]. This specific arrangement leads to strong antiferromagnetic ordering below the Néel temperature, a key feature of its magnetic behavior. In addition, CuO has been widely studied for its potential use in photocatalysis, gas sensing, and battery electrodes due to its high stability and environmental friendliness.

The unique combination of its structural, electrical and magnetic properties makes CuO an object of interest for both fundamental research and technological applications.

Figure I.4 shows the structure of CuO, where the copper ions (Cu²⁺) are coordinated by oxygen (O²⁻) in a distorted square planar or octahedral geometry, which gives CuO its unique electronic and magnetic properties.



Cubic

Figure I.4: CuO structure as crystallizes [16].

Red spheres probably represent oxygen (O) atoms, brown spheres probably represent copper (Cu)

atoms. The structure consists of Cu atoms in a cubic arrangement with O atoms around them in a tetrahedral coordination.

B. Stability properties

Stability of CuO can be considered in terms of thermal and chemical stability:

1. Thermal stability

Copper (II) oxide (CuO) exhibits thermal stability under typical conditions. While it will decompose to copper(I) oxide (Cu₂O) and oxygen via a disproportionation reaction at temperatures above 1026°C, this inherent high thermal stability makes it well suited for applications involving high temperature processes.

2. Chemical stability

CuO has good chemical stability. It is insoluble in water and shows resistance to corrosion. When heated, it behaves as a stoichiometric compound, maintaining its composition without significant loss of oxygen. This stability makes it a suitable catalyst in organic synthesis, especially in reactions that require robust and stable materials. These properties support its use in various applications, including the manufacture of ceramics, as a pigment in glasses, and in the synthesis of other copper salts.

I.4.2. Electronic and optical properties of CuO material

Copper oxide (CuO) possesses interesting electronic and optical properties, stemming from its semiconducting nature and its interactions with electromagnetic radiation across a range of energies.

A. Electronic properties

Copper oxide (CuO) is identified as a p-type semiconductor with a limited band gap, typically in the range of 1.2 to 2.0 eV, although this range may vary depending on the technique used for measurement and the purity of the sample [17]. The valence band maximum consists mostly of oxygen 2p orbitals, while the conduction band minimum consists mostly of copper 3d states. This electronic structure gives rise to strong electron correlation effects, resulting in the characteristic Mott insulator behavior of CuO.

The electronic structure of CuO, characterized by strong electron-electron and electron-phonon interactions, leads to a variety of physical phenomena.

B. Optical properties

Optically, copper (II) oxide (CuO) exhibits strong absorption in the visible light region, which accounts for its characteristic black to brownish-black appearance in powder form.

This absorption property is exploited in solar energy applications, where CuO can serve as an absorbing layer in photovoltaic cells [18].

In addition, CuO thin films have demonstrated significant photoconductive behavior, i.e., their electrical conductivity changes upon exposure to light. This property is valuable for optoelectronic devices.

I.4.3. Mechanical and thermal properties of CuO material

When discussing materials such as copper (II) oxide (CuO), it is essential to consider their mechanical and thermal properties, as these critical parameters determine their suitability for various applications.

A. Mechanical properties

Copper (II) Oxide (CuO) is a ceramic material with high hardness and moderate fracture toughness. Its Young's modulus (a measure of stiffness) and hardness are influenced by grain size and defect density; higher defect densities can reduce the effective hardness. While hard, CuO is also brittle, a typical characteristic of ceramic materials.

B. Thermal properties

The thermophysical behaviour of CuO is highly influenced by its nanostructure. At the nanoscale, CuO exhibits reduced thermal conductivity due to increased phonon scattering at grain boundaries and surfaces. This is beneficial for thermoelectric applications, as low thermal conductivity is required to maintain a temperature gradient. For example, thin films or nanostructured CuO materials have an even lower thermal conductivity than bulk CuO, which improves their performance in terms of thermal insulation and energy conversion. Combined with its chemical stability, these thermal characteristics support its use in solar thermal collectors, gas sensors, and lithium-ion batteries [19].

Copper oxide (CuO) is a p-type semiconductor that exhibits notable thermal properties critical for its use in electronics and energy devices. It has a relatively high melting point of around 1,320°C and a thermal conductivity of approximately 17 W/m·K at room temperature. While this is relatively low compared to metals, it is typical for semiconducting oxides. It has a specific heat capacity of around 0.53 J/g·K and good thermal stability, making it suitable for high-temperature applications. These thermal properties influence CuO's performance in photovoltaic and thermoelectric systems, where heat resistance and controlled thermal transport are essential. CuO also has a thermal expansion coefficient of around $10\text{--}12 \times 10^{-6}/\text{K}$, indicating moderate dimensional changes under thermal stress.

I.5. In-depth analysis of Cu₂O material

I.5.1. Structure and stability of Cu₂O material

Copper(I) oxide (Cu₂O) is an intriguing p-type semiconductor with a cubic crystal structure. Its inexpensive synthesis and unique properties make it useful in a wide variety of applications.

A. Structure properties

It forms a cubic structure with a Cu₂O lattice and a Pn3m space group. The structure can be thought of as a simple cubic arrangement of anions, with half of the cubic sites filled with cations.

(see Figure I.7).

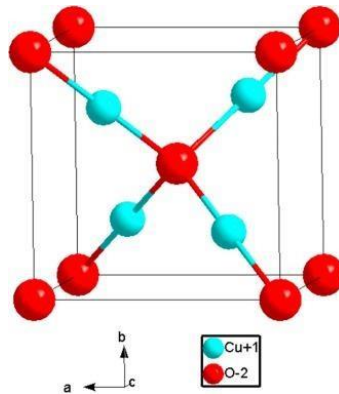


Figure I.5: illustrates the cubic structure of Cu₂O [20]

In this arrangement, each copper atom is in the center of a tetrahedron, with oxygen atoms occupying the vertices. The unit cell consists of two Cu₂O molecules.

B. Stability properties

Cu₂O is relatively stable under ambient conditions, but can decompose in moist air by oxidation to copper(II) oxide (CuO). It remains stable up to about 1230°C, but if heated above this temperature, it decomposes into copper metal and oxygen gas. Exposure to light can induce photo-corrosion in Cu₂O, leading to material degradation and compromising its structural integrity.

According to the rules of thermodynamics, Cu₂O is stable over a wide range of oxygen pressures and temperatures, contributing to its natural occurrence as the mineral cuprite.

I.5.2. Electronic and optical properties of Cu₂O material

Copper(I) oxide (Cu₂O) is valued for its unique electronic and optical properties, making it a valuable material in various electronic and optoelectronic applications.

A. Electronic properties

Cu₂O functions as a p-type semiconductor characterized by a direct band gap, a property that makes it suitable for use in semiconductor devices. Its band gap, approximately 2.0 to 2.2 eV, allows the material to absorb visible light. This property is used in various applications, including photovoltaic cells. The high hole mobility in Cu₂O also contributes to its usefulness in electronics, where efficient charge transport is essential. [21].

B. Optical properties

Cu₂O has a strong exciton binding energy, which allows exciton formation even at room temperature and contributes to its high optical absorption coefficient. These excitons are also responsible for the photoluminescence observed in Cu₂O, which can be exploited in applications such as light-emitting diodes (LEDs).

I.5.3. Mechanical and thermal properties of Cu₂O material**A. Mechanical properties**

Cu₂O, with a Mohs hardness of approximately 3.5 to 4, is considered relatively soft and therefore not ideal for applications requiring high wear resistance.

It has a moderate modulus of elasticity, suggesting a reasonable degree of stiffness and rigidity for a semiconductor[22].

B. Thermal properties

- ❖ Cu₂O's melting point of approximately 1235°C (2255°F) allows it to withstand high temperatures, but also limits its use in environments that exceed this limit.
- ❖ The specific heat capacity of Cu₂O is within the range expected for semiconducting oxides, reflecting its ability to absorb heat.
- ❖ Like most materials, Cu₂O undergoes thermal expansion, and its coefficient of thermal expansion is a critical consideration in applications subject to significant temperature variations.
- ❖ Thermal Conductivity: Cu₂O has relatively low thermal conductivity
Thermal Expansion: Cu₂O exhibits negative thermal expansion, meaning that it contracts when heated within certain temperature ranges.
- ❖ Thermal Expansion: Cu₂O exhibits negative thermal expansion, meaning that it contracts when heated within certain temperature ranges.
- ❖ Heat capacity: The heat capacity (C_p) of Cu₂O increases with temperature.
- ❖ These thermal properties make Cu₂O an interesting material for applications in thermoelectric devices and as a potential photocatalyst for environmental remediation

I.6. In-depth analysis of ZnO material**I.6.1. Structure and stability of ZnO material****A. Structure of ZnO**

Zinc oxide is composed of oxygen and zinc atoms with the formula ZnO. Zinc oxide has three

different crystallographic phases: the blende phase, the rock salt phase, and the wurtzite phase. The crystallization process has been studied according to the hexagonal close-packed structure of the wurtzite type.

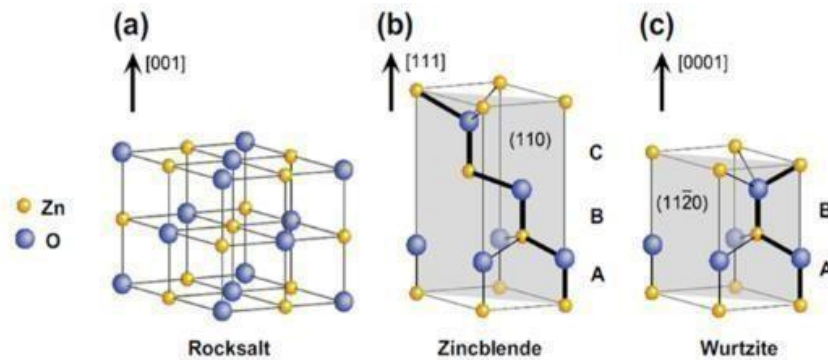


Figure I.6: Unit cell structure of Zinc oxide [23]

Under ambient conditions, the wurtzite structure is characterized as the most thermodynamically stable structure. The wurtzite structure can undergo a phase transition to a rock salt structure when subjected to elevated pressures. However, under decompression, the rock salt does not revert to the wurtzite structure at room temperature, but only at elevated temperatures [24].

B. Stability properties

Zinc oxide (ZnO) is a generally stable compound, but its stability can be affected by several factors:

1. Thermal stability

Zinc oxide is thermally stable at room temperature and under normal atmospheric conditions. It sublimates (changes directly from a solid to a gas) at approximately 1975°C. When heated in air, it may exhibit a thermal color change from white to yellow due to a slight loss of oxygen. This change is reversible on cooling.

2. Chemical stability

- **Insoluble in water:** ZnO is practically insoluble in water.
- **Amphoteric:** It reacts with both acids and bases.

Acids: Dissolves in most acids to form zinc salts. For example, with hydrochloric acid: $\text{ZnO} + 2 \text{HCl} \rightarrow \text{ZnCl}_2 + \text{H}_2\text{O}$

Bases: Reacts with strong bases to form zincates.

- **Reducing agents:** Can be reduced to zinc vapor by heating with carbon at high temperatures (around 950°C): $\text{ZnO} + \text{C} \rightarrow \text{Zn (vapor)} + \text{CO}$
- **Reactions with fatty acids:** Responds gradually with fatty acids found in oils to generate

carboxylates.

I.6.2. Electronic and optical properties of ZnO material

A. Electronic properties

Zinc oxide (ZnO) is a prominent semiconductor material with remarkable electronic properties that make it highly useful in various technological applications. It is known for its wide direct band gap (~3.37 eV at room temperature).

The various electrical properties of zinc oxide have been studied for a long time, which has allowed it to have a wide range of applications, but the low values of the carrier mobility do not allow it to compete in the field of electrical components. However, this problem has now been solved by Eagle-Picher, where mobilities of the order of 200 cm²/V.s at 300 K have been obtained [25].

B. Optical properties

Zinc oxide is a transparent material in the visible and near infrared due to its large optical gap (\approx 3.3 eV), its refractive index in solid form is equal to 2 and its absorption threshold is close to 380 nm. Furthermore, in the form of thin films, its refractive index (varying between 1.7 and 2.20) and its absorption coefficient vary depending on the processing conditions. Improving the stoichiometry of ZnO leads to a decrease in the absorption coefficient and an increase in the optical gap energy.

I.6.3. Mechanical and thermal properties of ZnO material

A. Mechanical properties

Zinc oxide (ZnO) is a mechanically robust semiconductor with high hardness, mechanical strength, and piezoelectric properties. Its high thermal stability, good wear resistance, and excellent mechanical durability make it a valuable material in coatings, sensors, ceramics, and optoelectronic devices

B. Thermal properties

Zinc oxide (ZnO) is a versatile semiconductor material with exceptional thermal properties that make it suitable for a wide range of applications. It has high thermal stability, which allows it to maintain its structural and chemical integrity at elevated temperatures [26].

This scientific graph shows the heat capacity (C_v) of various crystal structures of a material as a function of temperature, ranging from 300 K to 1500 K, with the units for heat capacity being J mol⁻¹ K⁻¹.

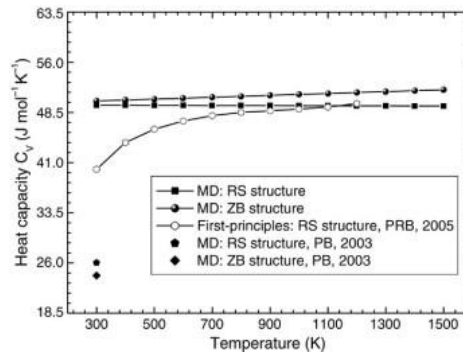


Figure I.8: MD-calculated constant-volume heat capacity of the ZnO with RS-type and ZB-type cubic structures, respectively [27].

MD: RS structure – molecular dynamics results for the rocksalt (RS) structure (black squares).

MD: ZB structure – molecular dynamics results for the zinc blende (ZB) structure (black circles).

First-principles: RS structure, PRB, 2005: Ab initio calculation results for the RS structure from a 2005 Physical Review B paper (open circles).

MD: RS structure, PB, 2003: Earlier molecular dynamics results for the RS structure from a 2003 Physics B publication (black diamond).

MD: ZB structure, PRB, 2003: Earlier MD results for the ZB structure (black triangle).

The heat capacity (C_v) remains relatively constant with increasing temperature for both the MD: RS and MD: ZB structures, hovering around $48.5\text{--}49.5\text{ J mol}^{-1}\text{ K}^{-1}$.

First-principles calculations (open circles) for the RS structure show a gradual increase in C_v from $\sim 41\text{ J mol}^{-1}\text{ K}^{-1}$ at 300 K to $\sim 48\text{ J mol}^{-1}\text{ K}^{-1}$ at 1500 K.

The 2003 MD data for both the RS and ZB structures (diamonds and triangles) are consistent with the newer MD data.

The RS and ZB structures (MD results) converge to similar heat capacity values at high temperatures (approximately $48.5\text{ J mol}^{-1}\text{ K}^{-1}$), suggesting little structural dependence at higher thermal energy levels.

The heat capacity at constant volume (C_v) shows minor temperature dependence for both the RS and ZB structures above $\sim 600\text{ K}$.

First-principles calculations suggest stronger temperature dependence at lower temperatures, but eventually converge with the MD results.

Convergence of all datasets near $48.5 \text{ J mol}^{-1} \text{ K}^{-1}$ supports the Dulong–Petit limit, theoretically expected for solids at high temperatures.

Overall, the RS and ZB structures behave similarly in terms of heat capacity at elevated temperatures, which is important for high-temperature applications.

I.7. Applications of CuO/ZnO heterojunction

- **Gas sensor:** Studies have shown that the CuO-ZnO nanocomposite exhibits excellent gas sensing capabilities. For example, Yang et al. used synthesized CuO-ZnO hybrids as p-type gas sensors, especially for the detection of reducing gases such as acetone, ethanol, and xylene.
- **Solar cell:** Using CuO-ZnO nanocomposite in solar cell applications has been investigated by several researchers. reported varying conversion efficiencies for CuO-ZnO-based solar cells. Their findings indicated efficiencies of $1.1 \times 10^{-4}\%$, 0.41%, 1.52%, and 0.1%, respectively, highlighting differences in performance based on fabrication methods and material properties.
- **Hydrogen generation:** Liu and colleagues explored the hydrogen production potential of the CuO-ZnO nanocomposite when used in a mixture of methanol and water. Their research indicated a hydrogen output of 1700 $\mu\text{mol/h}$ for every gram of the CuO-ZnO catalyst, surpassing numerous other semiconductor oxide catalysts in terms of effectiveness.
- **Humidity sensor:** Ashok et al. investigated the application of the CuO-ZnO nanocomposite as a humidity sensor.. Their findings indicated that the sensor exhibited enhanced sensing performance as the operating temperature increased from 500°C to 600°C, demonstrating improved sensitivity and response characteristics.

I.8. Applications of Cu₂O /ZnO heterojunction

- **Photovoltaic Cells (Solar Cells):** The Cu₂O/ZnO heterojunction, formed by combining p- type Cu₂O and n-type ZnO, plays a crucial role in thin-film solar cells. This structure optimizes light absorption and enhances charge separation, ultimately boosting the efficiency of energy conversion.
- **Photocatalysis and Self-Cleaning Surfaces:** Cu₂O/ZnO heterojunctions demonstrate high photocatalytic activity, making them effective for breaking down organic pollutants. Their application in glass surface treatments provides self-cleaning properties, improving surface functionality.

- **Self-Powered Photodetectors:** These heterojunctions are widely used in self-powered photodetectors, where the built-in electric field facilitates efficient charge separation without requiring an external power source. This significantly enhances light detection capabilities.

- **Plasmonic Photocatalysis:** The integration of plasmonic copper nanoparticles into the Cu₂O/ZnO heterojunction significantly improves photocatalytic performance.

The localized surface plasmon resonance phenomenon enhances light trapping and increases the efficiency of catalysis.

I.7. Conclusion

oxide (The exploration of copper oxide (CuO, Cu₂O) and zinc ZnO). in this chapter has highlighted their different physical, chemical, electronic and mechanical properties, demonstrating their significance in advanced material science. These metal oxides, with their unique semiconductor characteristics, have found widespread applications in renewable energy, optoelectronics, sensing technologies, and environmental protection.

As research in nanotechnology and material engineering advances, optimizing the synthesis, doping strategies, and heterostructure design of these oxides will unlock even greater potential in emerging fields such as flexible electronics, self-powered sensors, and energy-efficient devices.

Chapter II

Presentation of SCAPS-1D

simulator

II.1. Introduction

The advancement and refinement of solar cell technology depends on accurate simulation tools that allow researchers to evaluate their performance under different conditions. One of the most commonly used programs for this purpose is SCAPS-1D (Solar Cell Capacitance Simulator), a numerical modeling software developed by the Electronics and Information Systems Department (ELIS), Ghent University, Belgium[28]. Originally designed for use with thin-film solar cells such as CuInSe_2 and CdTe , its functionality has been extended to support other photovoltaic technologies, including silicon (Si), gallium arsenide (GaAs), and amorphous silicon (a-Si)[29].

SCAPS-1D provides a robust platform for simulating carrier transport, recombination dynamics, and both optical and electrical properties of solar cells. With tools such as batch calculations, recorder simulations, and curve fitting, researchers can systematically study the influence of various parameters on solar cell efficiency.

This chapter covers the core features of SCAPS-1D. It explains how to set operating points, run batch simulations, and fine-tune device characteristics using curve fitting methods.

II.2. The basics

SCAPS is Windows-based software developed using LabWindows/CVI from National Instruments. In this context, the term "panel" follows LW/CVI terminology, which may correspond to terms such as "window", "page", or "popup" in other software. When SCAPS is started, it first displays the Action Panel.

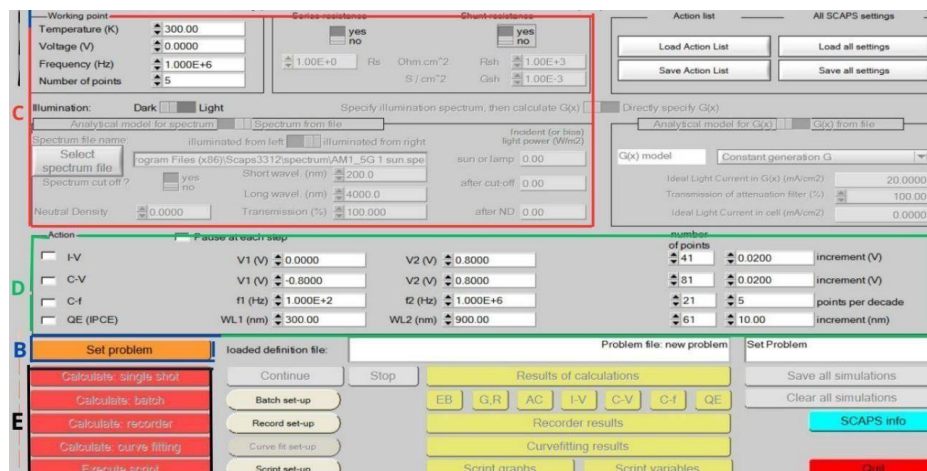


Figure II.1: Main Software User Interface.

SCAPS provides specialized panels for essential operations (see Figure II.1) , including:

- Running SCAPS to initiate the simulation.

- Define the problem, which includes defining the geometry, materials, and all relevant properties of the solar cell.
- Specify working conditions, including parameters for simulation.
- Selecting the desired calculations, indicating which measurements will be simulated.
- Executing the simulations by starting the calculations.
- Displaying the results, such as simulated curves and related data (refer to Section E for details).

II.2.1. To start SCAPS

- Click the SCAPS icon on the desktop.
- Double-click the scaps3200.exe file (or any other available SCAPS version) in the file manager.
- Once started, SCAPS will open with the Action Panel as the default interface.

II.2.2. Define the problem

- SCAPS (Solar Cell Capacitance Simulator) is a numerical simulation tool used to model and analyze semiconductor solar cells, especially thin-film and multi-junction structures. The primary problem that SCAPS addresses is the simulation of the electrical and optical behavior of solar cells in order to optimize their performance (see Figure II.2).

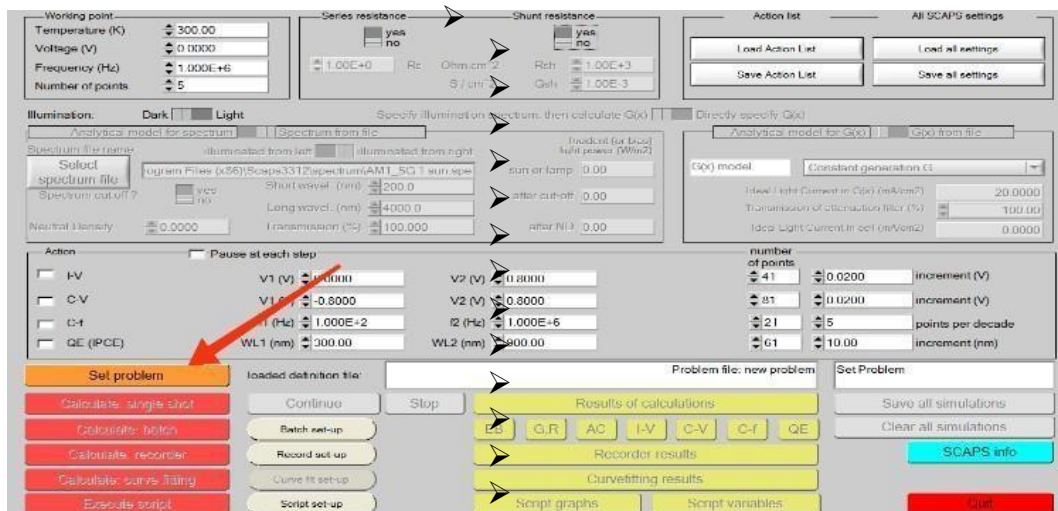


Figure II.2: Problem Definition Icon.

- In the Action Panel, click the Set Problem button.

- In the newly opened panel, select "Load" from the lower right corner.

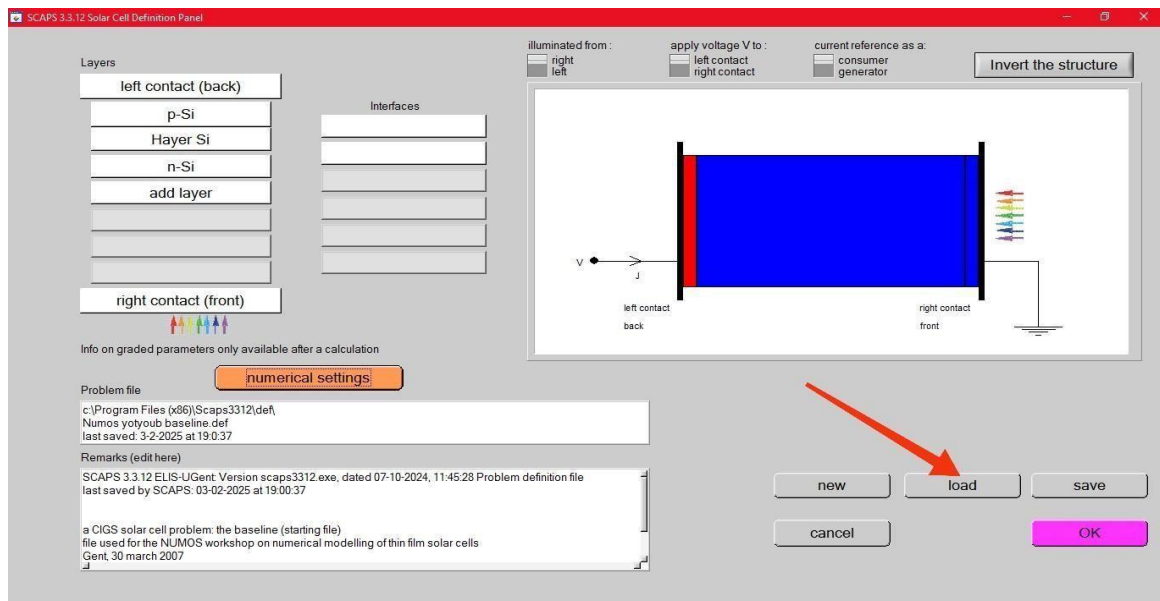


Figure II.3: File Uploading Feature Icon.

- Select and open a predefined problem file like NUMOS CIGS baseline.def, used as example from NUMOS workshop (Ghent, March 30, 2007).
- This file is usually located in the /scaps/def folder in the directory where SCAPS is installed. Browse to find it if necessary.
- At any time, you can change any of the solar cell properties by clicking "Set Problem" in the Action Panel.

II 2.3. Define the working point

The Working Point is the setting used to determine the parameters that remain the same during a measurement simulation. These parameters are important for the specific analysis. These parameters include:

Temperature (T):

- Essential for all measurements.
- In SCAPS, the clear influence of temperature affects solely $NC(T)$, $NV(T)$, thermal speeds, thermal voltage (kT), and their derivatives.
- Material parameters corresponding to each temperature must be manually input.

Voltage (V):

- Overlooked in I-V and C-V analyses.
- Functions as the DC-bias voltage during C-f and $QE(\lambda)$ analyses.

- SCAPS consistently begins at 0 V and modifies to the operating voltage by user-specified increments.

Frequency (f):

- Not taken into account in the I-V, $QE(\lambda)$ and C-f simulations.
- Not considered in I-V, $QE(\lambda)$, and C-f simulations.

Figure II.4: Device Operating Point Display.

Illumination:

Applied to all measurement types.

- In $QE(\lambda)$ simulations, it determines bias light conditions (e.g., dark or light).
- Users can choose the illuminated side and the spectrum for simulations.
- Default configuration: One Sun brightness (1000 W/m^2) utilizing the Air Mass 1.5 Global (AM1.5G) spectrum.

Figure II.5: Illumination Settings Section.

II 2.4. Select the measurement(s) to simulate

In the Action Panel, you can select one or more measurement types to simulate, including:

- I-V (Current-Voltage) Characteristics
- C-V (Capacitance-Voltage) Analysis
- C-f (Capacitance-Frequency) measurements

- QE(λ) (Quantum Efficiency as a function of wavelength)

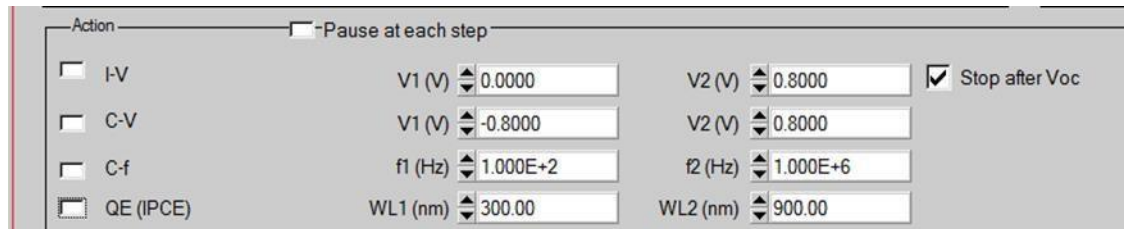


Figure II.6: Simulation Measurement Type Options.

Set Up the Simulation

- Navigate to the Action Panel and select the measurement(s) you want to perform.
- Adjust the start and end values for the selected parameter(s), if necessary.
- Define the number of steps for the simulation.

Tips for Efficient Simulations:

- Start with one simulation at a time and use coarse step sizes to avoid excessive computation time.
- When running a C-V simulation, note that the I-V curve is also generated automatically - it does not need to be selected separately.

II 2.5. Start the calculation(s)

In the Solar Cell Capacity Simulation (SCAPS) software, the "One-Shot" option in the Actions panel typically refers to running a single, complete simulation based on the current settings and parameters without repeating or scanning multiple conditions.

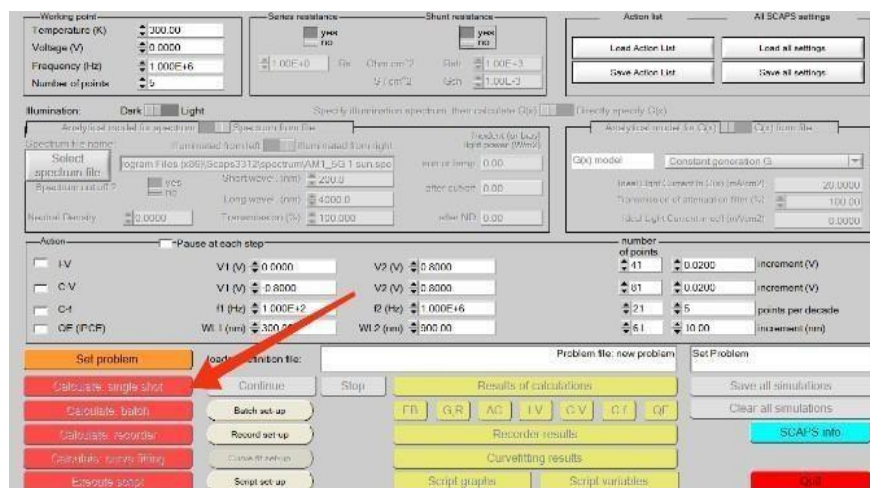


Figure II.7: Single-Shot Calculation Button.

The One-Shot Function in the SCAPS Actions Panel:

Runs a single simulation using the specified material settings.

Does not make any parameter changes (such as stress scan, temperature dependence, etc.).

Useful for obtaining quick results from a single set of conditions without repetition.

To begin the calculations, follow these steps:

- Click "Calculate: Single Shot" in the Action Panel.

Testing a single I-V (current-voltage) or QE (quantum efficiency) characteristic, Single Shot is the easiest for quick testing.

The Energy Bands panel opens and the simulation starts.

A status bar at the bottom of the panel shows the progress, e.g., "IV from 0.000 to 0.800 volts:

V = 0.620 Volt", indicating the current stage of the simulation.



Figure II.8: Simulation Current Stage Display.

SCAPS visually displays the evolution of key parameters such as:

- Conduction and valence bands
- Fermi levels
- Other relevant electronic properties

II 2.6. Display the simulated curves

When the calculations are complete, SCAPS automatically switches to the Energy Band Panel or AC Band Panel. Here you can analyze key results, including:

- Band Diagrams

➤ Carrier Densities



Figure II.9: Power Range Curve Panel.

II 2.6.1. Control panel data output options in SCAPS

- The output options include the following:
- Prints results.
- Save graphs for further analysis.
- Show numerical data on screen (enables cut & paste into external software like Excel).
- Saves numeric data to a file.
- Once you have simulated a measurement, you can switch to one of the specialized output panels, such as the I-V panel, for further visualization and analysis.

SCAPS (Solar Cell Capacitance Simulator) provides several options for exporting and visualizing simulation results. These options allow users to save and analyze data from different types of simulations, including I-V, C-V, QE, band plots, and carrier densities.

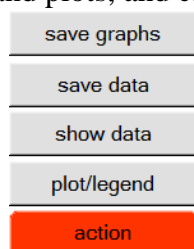


Figure II.10: Data Output Control Options.

Data output handling buttons:

Save Graphs

Exports the currently displayed graphs as image files (e.g., PNG, BMP, or JPEG). Useful for inclusion in reports and presentations.

Save Data

Saves numerical data from simulations to text files (.txt, .dat, or .csv). Enables further processing in Excel, MATLAB, or Python.

View Data

Displays numerical data in a structured spreadsheet format within SCAPS.

Plot/Legend

Customizes the plot display, enabling or disabling legends for better visualization.

SCAPS provides comprehensive data output options through its control panel, allowing users to effectively analyze, store, and visualize solar cell performance.

II.3. Left contact

In the Solar Cell Capacitance Simulator (SCAPS), the left contact refers to the back contact of the solar cell.

If the Left Contact button is selected (see Figure II.10), its properties can be configured, including the velocity parameters for electrons and holes, as well as details regarding the output work function. Once the OK button is clicked, the entered data is saved and the Solar Cell Definition Panel reappears.

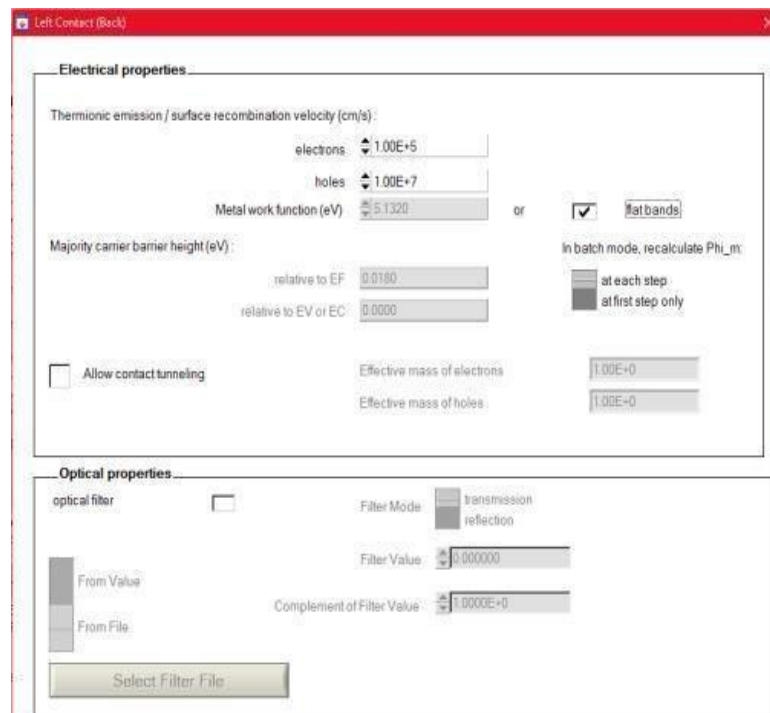


Figure II.11: Left Device Contact Window.

II.4. Right contact

In SCAPS (Solar Cell Capacitance Simulator), the right contact refers to the front contact of the solar cell, where the charge carriers exit the device. The Right contact is specified in the same way as the left contact.

II.5. Interface between layers

To specify the interface properties between two planes, click on the right side of the rectangle representing the planes. In addition, up to three types of defects can be configured using the "Defect1, 2, 3" button.

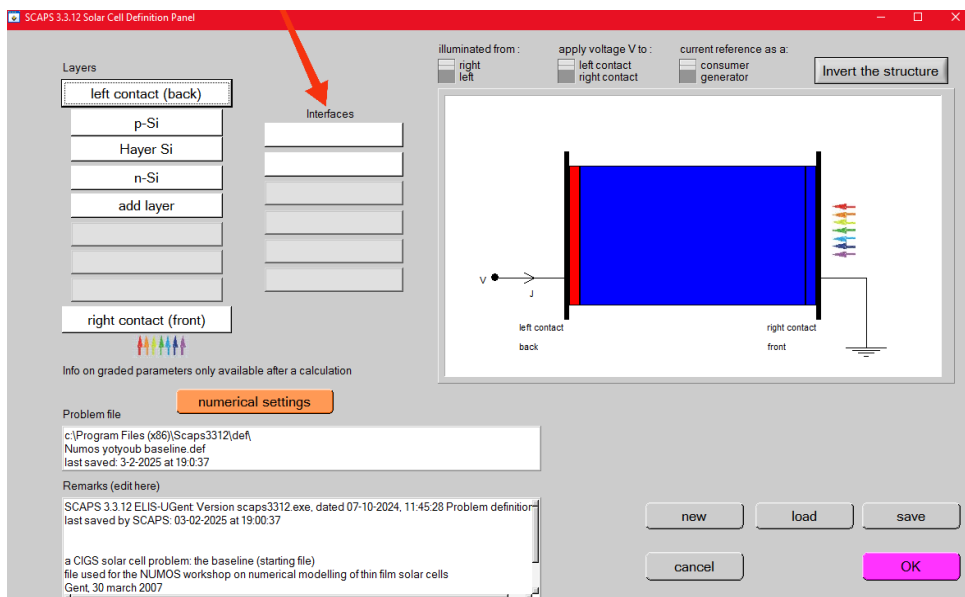


Figure II.12: The interface between the layers.

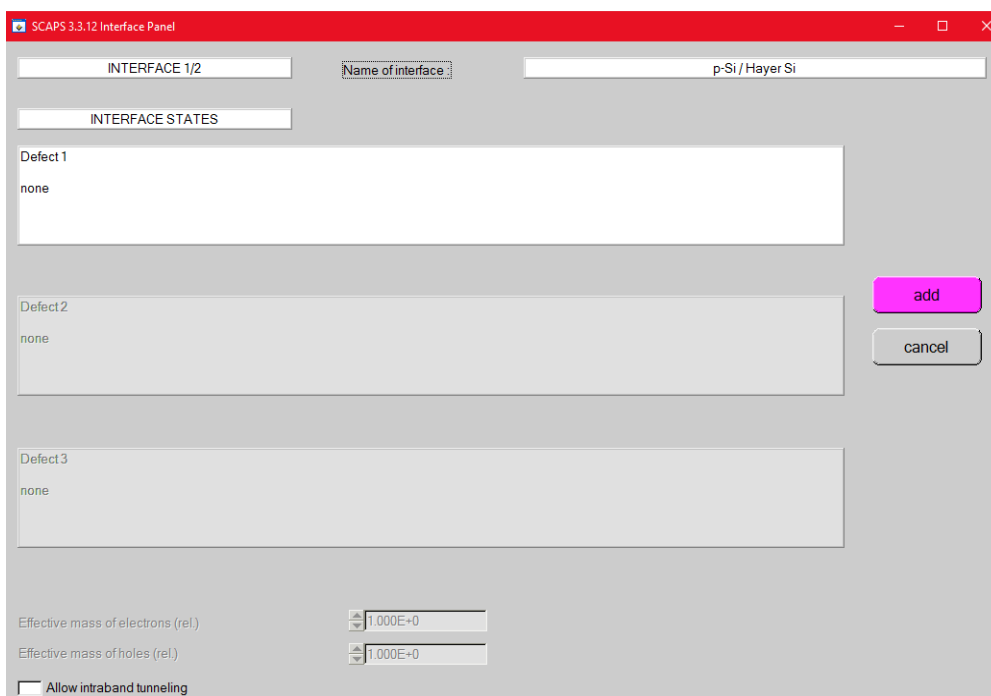


Figure II.12: Defect Settings Interface Panel.

Once the structure is fully defined, the configuration can be saved by clicking the "Save" button. Pressing "OK" completes the setup and opens the Energy Band Panel, which displays various graphical representations (see Figure II.12 and Figure II.13).

II.6. Conclusion

SCAPS-1D has proven to be an essential tool in photovoltaic research, providing a detailed and flexible framework for simulating solar cell behavior. By allowing users to define temperature, voltage, frequency, and illumination conditions, the software provides precise control over simulation settings.

The batch calculation and recorder feature further enhance its utility by facilitating multi-parameter analysis and tracking of results over different operating conditions. In addition, the curve fitting functionality helps bridge the gap between experimental data and theoretical models, ensuring that simulations reflect real-world solar cell performance. As photovoltaic technology continues to evolve, SCAPS-1D will remain a critical resource for researchers to develop more efficient and cost-effective solar energy solutions.

Chapter III

Results and Discussions

III.1. Introduction

Recent fundamental research has focused on semiconducting metal oxides[30] , with CuO and Cu₂O showing promise as absorber materials for optoelectronics and potentially enabling low-cost solar cell fabrication. Despite the theoretical efficiency limit of about 20% for Cu₂O solar cells[31], reported efficiencies on substrates have only reached 3.83% [32], indicating a need for further investigation. Since energy conversion efficiency is of paramount importance in photovoltaics[33], our work numerically investigates CuO and Cu₂O thin film solar cells using the SCAPS-1D program.

This simulation-based study aims to determine key photovoltaic parameters-open-circuit voltage (VOC), short-circuit current density (JSC), fill factor (FF), and efficiency (η)-under standard AM1.5G illumination (100 mW/cm², 300K). Specifically, we intend to analyze how variations in physical parameters such as thickness and acceptor concentration affect the performance of these solar cells, with a focus on the resulting short-circuit current density (JSC) and efficiency (η). In addition, we will evaluate the quantum efficiency (QE) of the simulated devices.

III.2. Modeling a copper oxide (CuO) and zinc oxide (ZnO) solar cell substrate

The conventional solar cell structure consists of a glass substrate as the back-absorber layer (CuO) and a transparent conductive zinc oxide (ZnO) front layer (Figure III.1). This structure is designed to enhance light absorption. In the conventional structure, a copper oxide (CuO) absorber layer is embedded in a p-type layer to form a high quality p-n junction at the interface. The copper oxide (CuO) layer was selected with a band gap of 1.200 eV, thicknesses of 0.5, 1.1, 1.5, and 2 μm , and an electron affinity of approximately 3.230 eV.



Figure III.1 : CuO solar cell structures.

III.3. Physical model and simulation parameters

Two semiconductor materials - copper oxide (CuO) and zinc oxide (ZnO) - were chosen to form a heterostructure for optoelectronic applications such as solar cells or photodetectors.

The properties of this cell are shown in Table III.1.

Table III.1: Parameters values of CuO and ZnO solar cell structures used in SCAPS-1D

Material properties	CuO	ZnO
Thickness	2	0.100
Band gap [eV]	1.200 *	3.370
Electron affinity [eV]	3.230	3.900
Dielectric permittivity (relative)	18.100 *	86
CB (conduction band) effective density of states [cm^{-3}]	3×10^{19} *	1.320×10^{20}
VB (valence band) effective density of states [$1/\text{cm}^3$]	5.500×10^{20} *	1.500×10^{21}
Electron mobility μ_n [cm^2/Vs]	0.1	10
Hole mobility μ_p [cm^2/Vs]	10	20
Shallow uniform donor density N_D [$1/\text{cm}^3$]	0	1×10^{19}
Shallow uniform acceptor density N_A [$1/\text{cm}^3$]	1×10^{16} *	0

* These values were updated from the reference [34].

These parameters include thickness w , bandgap E_g , electron affinity χ_e , electron/hole mobility μ_n/μ_p , effective conduction/valence band density of states N_C/N_V , and donor/acceptor concentration N_D/N_A , as they collectively determine the optical absorption, carrier transport, and junction properties that ultimately determine the performance and efficiency of the solar cell.

A comprehensive understanding of these parameters enables precise control of the electrical and optical properties of the solar cell, facilitating material selection, device design, and performance optimization to achieve high efficiency and reliability.

III.4. Band diagram

A band diagram is a graphical representation of the energy levels - specifically the conduction band and valence band - in a semiconductor device. It is critical for analyzing charge carrier behavior, junction formation, and internal electric fields in solar cells.

Figure III.2 shows two diagrams illustrating the electronic energy bands in a semiconductor structure. The horizontal axis in both plots represents the distance along the material, measured in micrometers (μm).

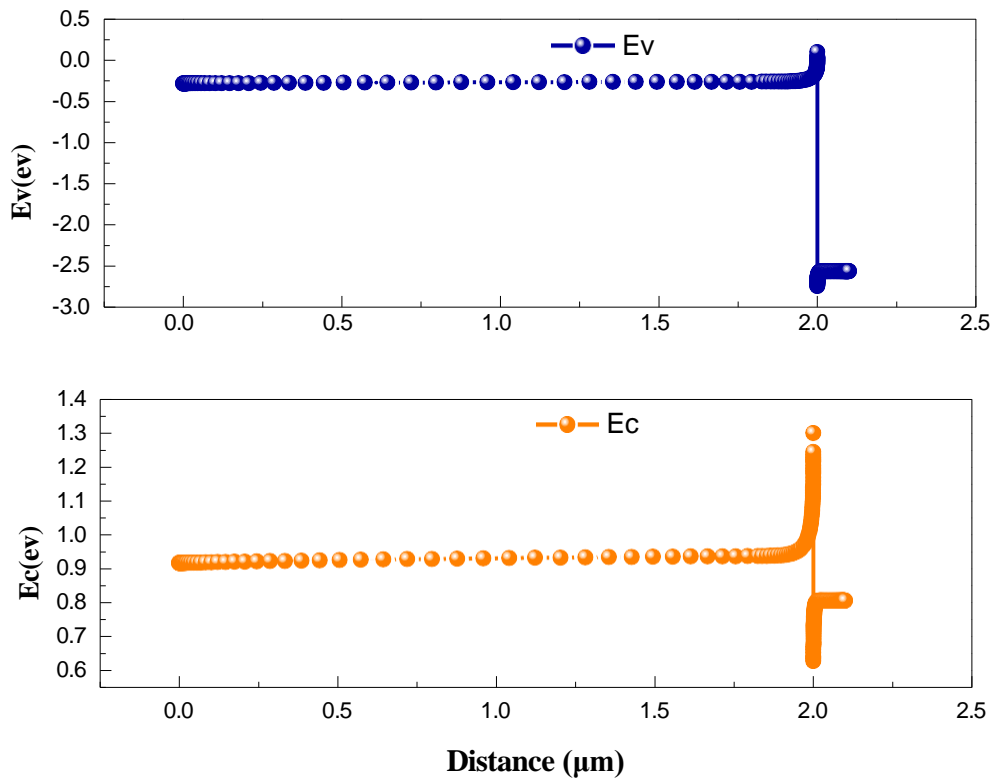


Figure III.2: Band diagram for CuO solar cells structures used in the simulation.

For most of the x axis (from 0 to just before 2.0), the energy valance band (E_v) is nearly constant and negative (about -0.5 eV), indicating a small internal electric field. Near $d \approx 2.0 \mu\text{m}$, there is a sharp decrease - the energy drops to about -2.8 eV and fluctuates. This is due to the formation of a built-in electric field due to Fermi level equilibrium. This also indicates a strong valance band shift, which is expected due to the difference in electron affinities and band gaps between ZnO and CuO. The energy conduction band (E_c) remains nearly constant between 0 and 2.0 μm at 0.9 eV due to equilibrium and the absence of applied bias. This flatness reflects a low internal electric field and uniform doping. At 2.0 μm , E_c reaches 1.3 V. there is a conduction band shift (ΔE_c) between CuO and ZnO, and then decreases rapidly to about 0.7 V. This is due to the presence of a built-in field, possible defects, or surface recombination at the front contact.

III.5. Thickness optimization of CuO absorber layer

In this section, we discuss the performance of a zinc oxide/copper oxide (ZnO/CuO) solar cell using the material parameters listed in Table III.1. Figure III.3 shows the evolution patterns of V_{oc} , J_{sc} , FF, and η for a CuO solar cell as a function of the thickness of the CuO absorber layer.

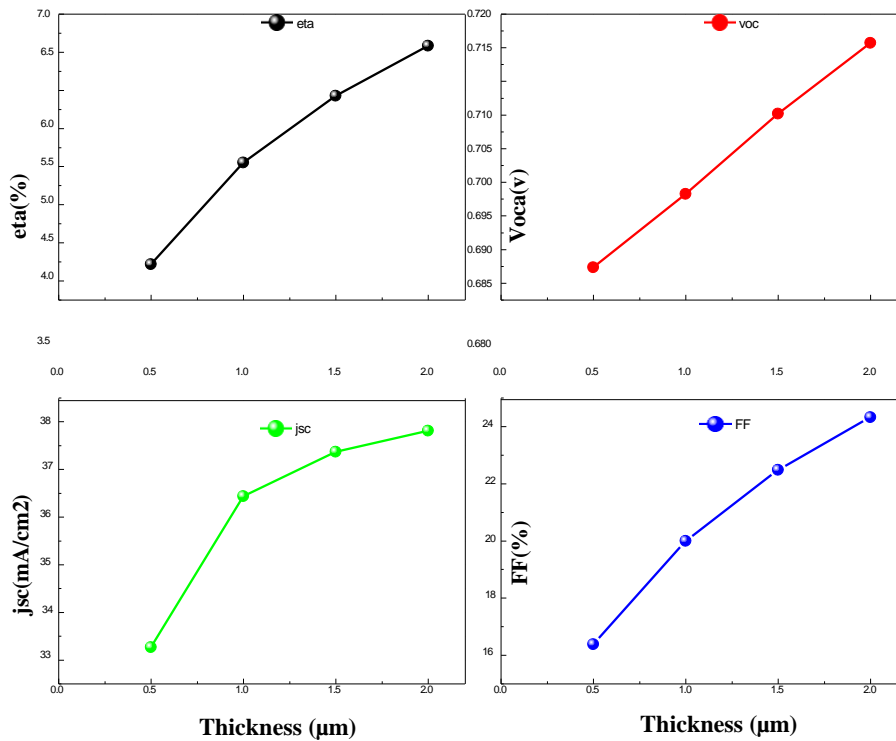


Figure III.3: Thickness of the CuO absorber

As the thickness of the CuO absorber layer (CuO) increases from 1 to 2 μm , J_{sc} increases significantly from 32.11 mA/cm² to about 37.15 mA/cm², and η increases rapidly from 5.24% to about 8.16%.

V_{oc} increases from 0.69 to 0.73 V, and FF reaches 31.33%, up from 23.37% previously. This overall behavior results from increased photon absorption and even increased electron gap generation in the CuO absorber layers.

Therefore, a thickness of 2 μm has been selected as the optimal thickness of the copper oxide (CuO) absorber layer for efficient ZnO/CuO solar cells. This knowledge is essential for the development of cost-effective and scalable solar energy technologies, especially with earth-abundant materials such as copper oxide.

III.6. Quantum efficiency QE

Based on previous studies, we selected a thickness of 2 micrometres as the best option. We then

measured the quantum efficiency and observed that it increased as the thickness increased.

The curve shown in Figure III.4 was obtained. See the figure. The graph shows the quantum efficiency (QE) as a function of wavelength (in nanometers, nm).

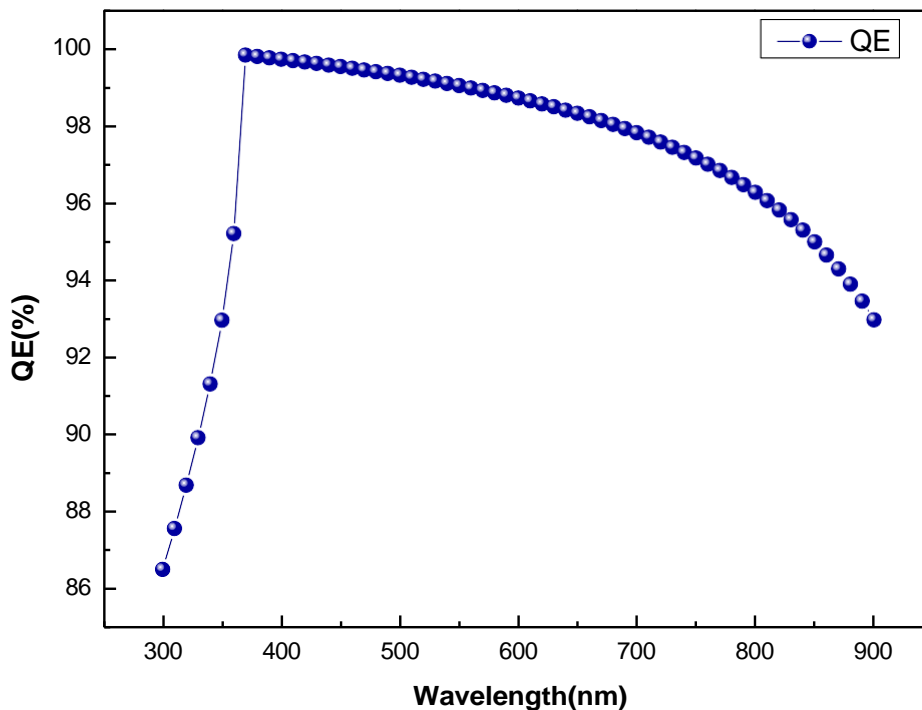


Figure III.4: Quantum efficiency versus wavelength of CuO solar cell structures.

The quantum efficiency starts at around 90% at 300–370 nm and gradually increases. Between 370 and 400 nm, it peaks at around 100% and remains constant. Between 400 and 650 nm, the quantum efficiency remains very high, decreasing slightly from 100% to approximately 97–98%. Between 650 and 900 nm, the quantum efficiency gradually decreases to approximately 92–93% at 900 nm. High quantum efficiency (around 100%) over a wide wavelength range indicates excellent device performance [35].

The slight decrease at longer wavelengths indicates minor recombination losses in the bulk, though performance remains excellent (>90%). High and stable quantum efficiency (QE) indicates good optical absorption and carrier transport properties, making it a critical metric for evaluating photovoltaic material performance. Quantum efficiency is higher in the 370–400 nm range than in other ranges because the quantum efficiency peaks at around 100% in this range.

III.7. Optimization of acceptor density NA(CuO)

It was found that the acceptor concentration of the copper oxide (CuO) absorber layer is an

important factor that directly affects the performance of solar cells. Therefore, the acceptor concentration was studied in terms of electrical properties (Figure III.5), which include efficiency (η), open-circuit voltage (V_{oc}), short-circuit current (J_{sc}), and fill factor (FF).

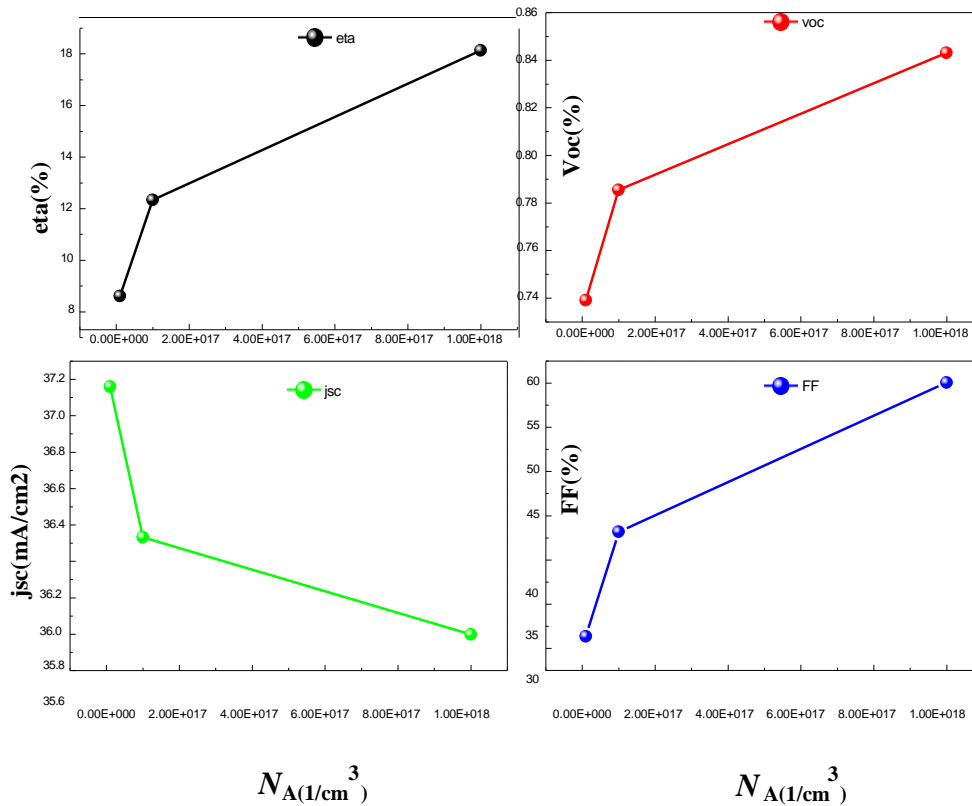


Figure III.5: acceptor concentration of absorber layer $N_A(\text{CuO})$ on cell performances.

The acceptor concentration of the absorber layer, $N_A(\text{CuO})$, was adjusted from 10^{16} cm^3 to 10^{18} cm^3 , and the simulated photovoltaic properties are shown in Figure III.6. The J_{sc} shows a decrease from 37.15 mA/cm^2 at a concentration of 10^{16} cm^3 to 35.79 mA/cm^2 at a concentration of $1 \times 10^{18} \text{ cm}^3$.

On the other hand, V_{oc} , FF and efficiency all increase as the $N_A(\text{CuO})$ concentration increases from 10^{16} cm^3 to 10^{18} cm^3 , with the optimum efficiency reached at 18.12%. In conclusion, the acceptor concentration of the $N_A(\text{CuO})$ absorber layer is favourable within this range (From 10^{16} cm^3 to 10^{18} cm^3).

III.8. Modeling a copper oxide (Cu_2O) and zinc oxide (ZnO) solar cell substrate

To design a $\text{Cu}_2\text{O}/\text{ZnO}$ solar cell, a Cu_2O layer acts as a back layer designed to absorb sunlight, and an n-type ZnO layer, which is transparent and electrically conductive, acts as the front layer. The idea behind this arrangement is to allow the Cu_2O to absorb the maximum amount of light and

then efficiently transfer the resulting electrical charges across the direct interface with the ZnO.

We set the Cu_2O thickness to a constant $2 \mu\text{m}$, the acceptor density to 10^{18} cm^{-3} , and the average bandgap to $E_g = 1.170 \text{ eV}$. We used zinc oxide with a thickness of $0.1 \mu\text{m}$ and a donor density of $1 \times 10^{19} \text{ cm}^{-3}$, with a bandgap of $E_g = 3.37 \text{ eV}$.

III.9. Physical model and simulation parameter

In order to form a heterogeneous structure, $\text{ZnO}/\text{Cu}_2\text{O}$ was formed according to certain properties and attached in Table III.2.

Table III.2: Parameters values of Cu_2O and ZnO solar cell structures used in SCAPS- 1D[36][37].

Material properties	Cu_2O	ZnO
Thickness	2	0.100
Band gap [eV]	1.170	3.370
Electron affinity [eV]	3.500	3.900
Dielectric permittivity (relative)	10.000	86.000
CB (conduction band) effective density of states [cm^{-3}]	2×10^{17}	1.320×10^{20}
VB (valence band) effective density of states [$1/\text{cm}^3$]	1.1×10^{18}	1.500×10^{21}
Electron mobility μ_n [cm^2/Vs]	200	10
Hole mobility μ_p [cm^2/Vs]	80	20
Shallow uniform donor density N_D [$1/\text{cm}^3$]	0	1×10^{19}
Shallow uniform acceptor density N_A [$1/\text{cm}^3$]	1×10^{18}	0

These parameters include thickness w , transmittance ϵ_r , band gap E_g , electron affinity χ_e , electron/gap mobility μ_n/μ_p , density of conduction/valence band effective states (N_C/N_V), and donor/acceptor concentration (N_D/N_A). In heterogeneous solar cells, parameters such as thickness w , transmittance ϵ_r , band gap E_g , electron affinity χ_e , electron/gap mobility μ_n/μ_p , density of conduction/valence band effective states (N_C/N_V), and donor/acceptor concentrations (N_D/N_A) are critical for optimizing device efficiency.

III.10. Band diagram

Figure III.6 shows two diagrams illustrating the electronic energy bands in a semiconductor structure. The horizontal axis in both diagrams represents the distance along the material, measured

in micrometers (μm).

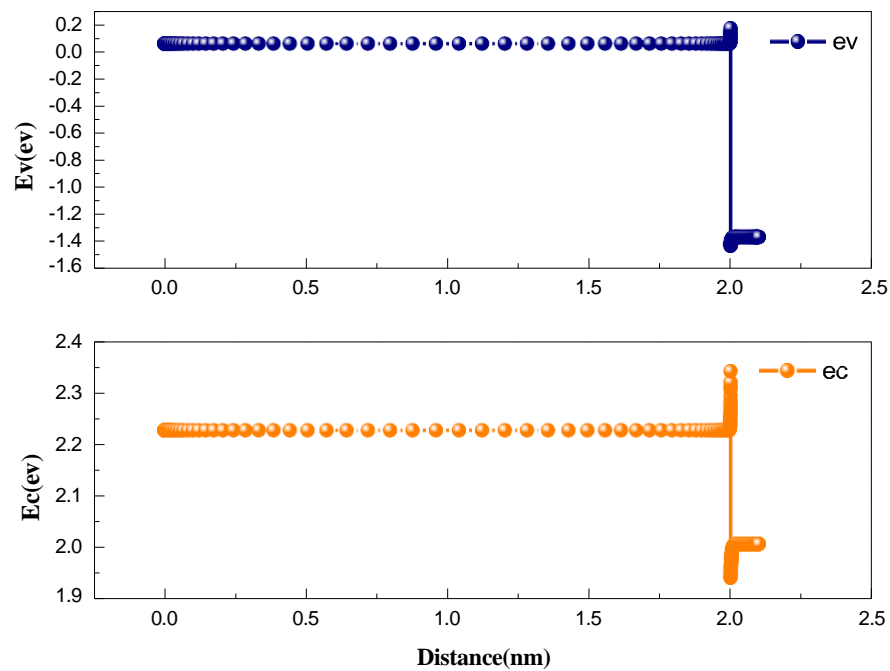


Figure III.6: Band diagram for Cu_2O solar cells structures used in the simulation.

From 0 to about 2.0 μm , the valence band energy (E_v) is nearly constant, indicating a small internal electric field, close to 0 eV. At around 2.0 μm , there is a sudden and sharp decrease in valence band energy to approximately -1.5 eV. This drop reflects the valence band shift ΔE_v characteristic of binary heterojunctions, in which the E_v value of zinc oxide ZnO is lower than that of copper oxide Cu_2O . This discontinuity results from differences in electron affinity (χ) and bandgap energies (E_g).

From 0 to about 2.0 nm, the conduction band energy (E_c) remains relatively constant at about 2.2 eV. Approaching 2.0 nm, there is a sudden drop in the conduction band energy to about 2.0 eV or slightly lower. This means that the conduction band of ZnO is lower than that of Cu_2O relative to the Fermi level, and ZnO has a band gap of about 3.3 eV and a strong electron affinity (about 3.9 eV), which affects the band bending and alignment.

III.11. Thickness optimization of Cu_2O absorber layer

To understand the relationship between film thickness and some of the basic electrical properties of a photovoltaic device, each property is presented in a separate graph as a function of thickness

(Figure III.7). The properties shown include efficiency (η), open-circuit voltage (V_{oc}), short-circuit current (J_{sc}), and fill factor (FF).

As film thickness increases, light absorption within the material generally improves, resulting in a higher short-circuit current (J_{sc}) due to the increased number of absorbed photons. However, there is a trade-off, as thicker films can lead to increased recombination losses, which can reduce open-circuit voltage (V_{oc}) and fill factor (FF). Efficiency (η) initially increases with thickness, but at a certain point, it may plateau or even decrease due to the balance between light absorption and recombination losses. These graphs help optimize device design by balancing the trade-off between increased current generation and potential losses in voltage and fill factor as thickness change.

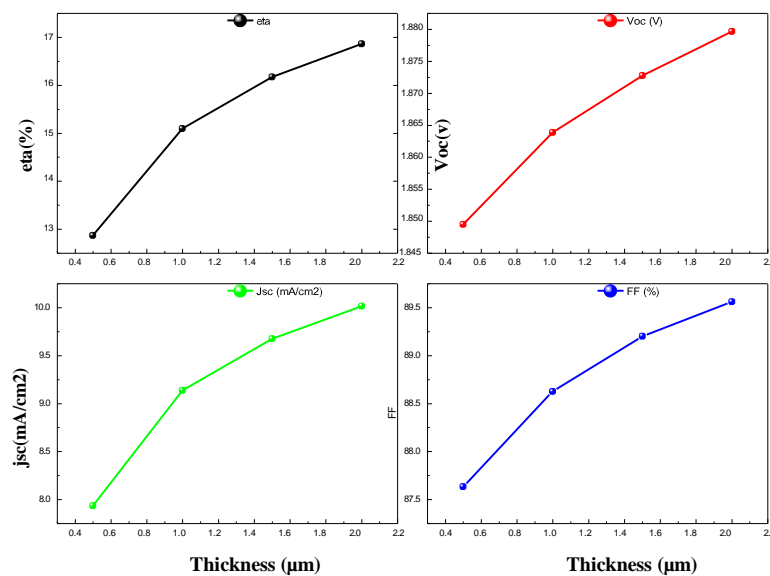


Figure III.7: Thickness of the Cu_2O absorber

As the thickness of the Cu_2O absorber increases from $0.5 \mu\text{m}$ to $2 \mu\text{m}$, the short circuit current density (J_{sc}) increases from $7.93 \text{ mA}/\text{cm}^2$ to $10.01 \text{ mA}/\text{cm}^2$, the efficiency (η) increases from 1.28% to 1.68% , and the open circuit voltage (V_{oc}) increases slightly from 1.84 V to 1.87 V . The fill factor (FF) also improves from 8.76% to 8.95% .

The importance of understanding these properties lies in their ability to guide design decisions and improve the performance of photovoltaic devices. This understanding is critical to scaling up solar cell production and designing devices that achieve high efficiencies while remaining cost-effective in terms of materials and manufacturing processes.

III.12. Quantum efficiency QE

This graph (Figure III.8) shows the quantum efficiency (QE) as a function of wavelength (in nanometers, nm).

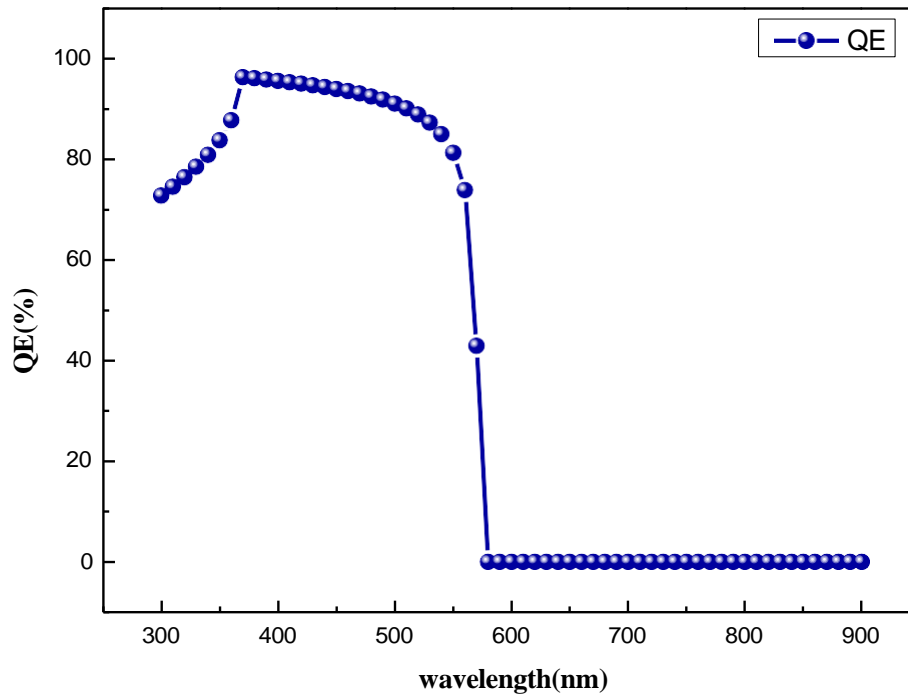


Figure III.8: Quantum efficiency versus wavelength of Cu_2O solar cell structures.

The quantum efficiency increases as the wavelength increases from approximately 300 nm to 400 nm. The quantum efficiency remains high and stable (close to 100%) in this range. Photon energies are still above the band gap, and the absorption coefficient is high. Electrons and holes are generated in regions with low recombination rates and are efficiently combined. Therefore, the quantum efficiency remains high, often approaching 100%. Beyond 550 nm, it drops rapidly to zero. This is due to the inability of photons to excite electrons from the valence band to the conduction band - no electron-hole pairs are formed and the quantum efficiency drops rapidly[38].

III.13. Optimization of acceptor density NA (Cu_2O)

At this stage, we will also study the change in acceptor concentration as a function of electrical properties such as efficiency (η), open circuit voltage (V_{oc}), short circuit current (J_{sc}), and fill factor (FF).

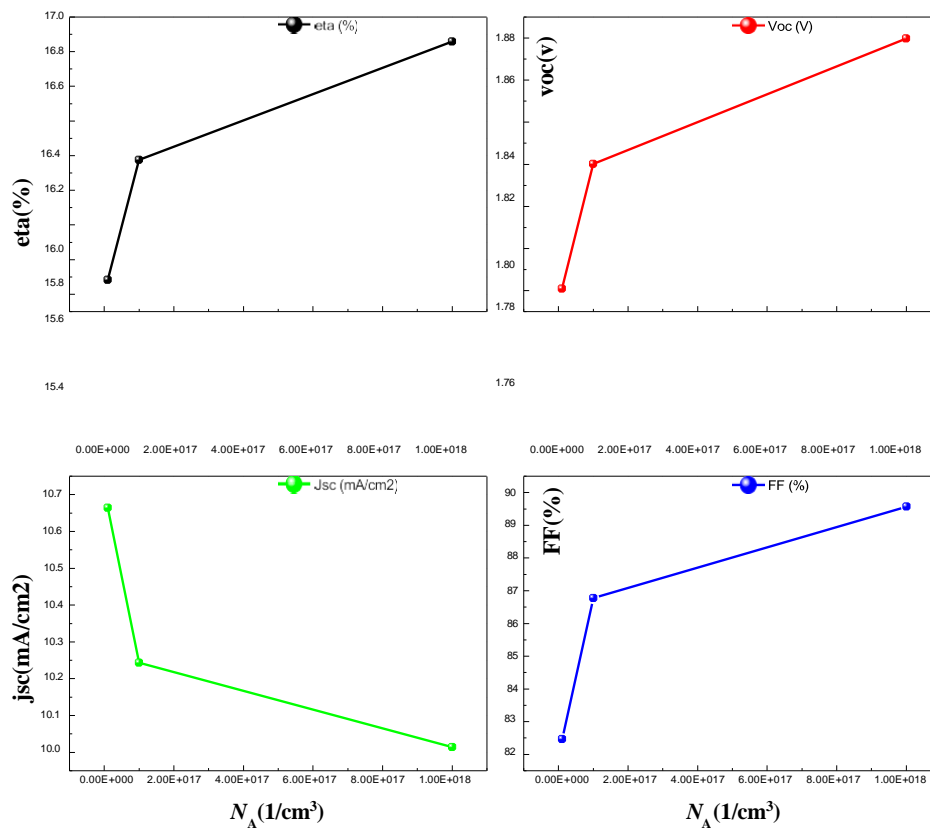


Figure III.9: acceptor concentration of absorber layer N_A (Cu_2O) on cell performances.

The acceptor concentration of the absorber layer, N_A (Cu_2O), was adjusted from 10^{16} cm^{-3} to 10^{18} cm^{-3} . Jsc shows a decrease from 10.66 mA/cm^2 at a concentration of 10^{16} cm^{-3} to 10.01 mA/cm^2 at a concentration of $1 \times 10^{18} \text{ cm}^{-3}$, and Voc, FF, and efficiency all increase with increasing N_A (Cu_2O) concentration from 10^{16} cm^{-3} to 10^{18} cm^{-3} , with the optimum efficiency reaching 16.85%.

III.14. Analysis of results

III.14.1. Thickness of CuO and Cu_2O

As the thickness of both CuO and Cu_2O increases, VOC, JSC, FF, and ETA all increase, indicating increased photon absorption and even increased electron-hole generation in the CuO and Cu_2O absorber layers. Therefore, a thickness of $2 \mu\text{m}$ was chosen as the optimal thickness for the CuO and Cu_2O absorber layers for efficient ZnO/CuO and ZnO/ Cu_2O solar cells.

III.14.2. Acceptor density N_A (CuO), N_A (Cu_2O)

The Jsc for both CuO and Cu_2O shows a very slight decrease from 37.15 mA/cm^2 at a concentration of 10^{16} cm^{-3} to 35.79 mA/cm^2 at a concentration of $1 \times 10^{18} \text{ cm}^{-3}$ and from 10.66 mA/cm^2 at a concentration of 10^{16} cm^{-3} to 10.01 mA/cm^2 at a concentration of $1 \times 10^{18} \text{ cm}^{-3}$, which is due to

the increased free carrier recombination occurring within the bulk. On the other hand, Voc, FF and efficiency increase with increasing NA, while the optimum efficiency is 18.12%, 16.85. Beyond this value, the structure shows a significant decrease in Voc, FF and efficiency. This result

indicates that the values of NA (CuO) and NA (Cu₂O) should be between 10^{16} cm^{-3} and $1 \times 10^{18} \text{ cm}^{-3}$ to achieve good performance.

III.15. Solar cell performance comparison

This work presents a comparative evaluation of the performance of Cu₂O/ZnO and CuO/ZnO solar cells based on simulation parameters, including open-circuit voltage (Voc), short-circuit current density (Jsc), fill factor (FF) and power conversion efficiency (η).

The aim is to provide a deeper understanding of the key physical limitations and practical design considerations for next-generation all-oxide solar cells. Our results aim to guide the optimisation of all-oxide solar cells by shedding light on the key parameters of open-circuit voltage (Voc), short-circuit current density (Jsc), fill factor (FF) and power conversion efficiency (η).

Other researchers have conducted simulations of CuO/ZnO and Cu₂O/ZnO cells and compared their results with ours to evaluate the quality of our simulations. This helps us to determine whether we can implement the cells in real-world applications or improve upon our own results if they are inferior to those of the simulations we are comparing with.

Tables III.3 and III.4 show the property values these researchers used in their simulations.

Table III.3: Properties of Materials used in our simulation[39].

Material properties	p-CuO	n-ZnO
Relative permittivity	18.1	86
Bandgap (eV)	1.2	3.37
Electron affinity (eV)	4.07	3.9
Effective density of states of valence band maximum(cm^{-3})	5.5×10^{20}	1.50×10^{21}
Effective density of states of conduction band minimum (cm^{-3})	3×10^{19}	1.32×10^{20}
Acceptor concentration(cm^{-3})	1×10^{16}	0
Donor concentration(cm^{-3})	0	1.00×10^{19}
Mobility of Hole ($\text{cm}^2/\text{V s}$)	10	20
Mobility of Electron ($\text{cm}^2/\text{V s}$)	0.1	10

Table III.4: Summary of the Properties of the Materials included in the numerical simulation wok[40].

Material properties	p-Cu ₂ O	n-ZnO
Bandgap (eV)	3.4	2.1
Electron Affinity (eV)	4.2	3.2
Dielectric Permittivity (relative)	9	7.6
Conduction Band Density of States (cm ⁻³)	2.2 x 10 ¹⁸	2.43 x 10 ¹⁹
Valence Band Density of States (cm ⁻³)	1.8 x 10 ¹⁹	1.1 x 10 ¹⁹
Electron Thermal Velocity (cm/s)	1.0 x 10 ⁷	1.0 x 10 ⁷
Hole Thermal Velocity (cm/s)	1.0 x 10 ⁷	1.0 x 10 ⁷
Electron Mobility (cm ² /Vs)	60	100
Hole Mobility (cm ² /Vs)	30	50

In our work we considered the characteristics listed in Tables III.1 and III.2. The results of these characteristics were compared with those of other individuals (see Tables III.5 and III.6).

Tables III.5 : Table showing previous study about CuO/ZnO simulation results and our results.

Parameter	Literature [41]	Our values
V _{oc} (V)	0.765 V	0.73 V
J _{sc} (mA/cm ²)	38.5 mA/cm ²	37.15 mA/cm ²
FF (%)	80.6%	31.33%
η (%)	23.6%	8.16%

The results presented show poorer performance, particularly in terms of Fill factor (FF): Significantly low (~31% vs. ~80%), indicating significant resistive or recombination losses. Efficiency (η): Significantly low (8.16% vs. 23.6%), mainly due to a lower fill factor and slightly lower V_{oc} and J_{sc}. V_{oc} and J_{sc} moderately lower than the ideal/simulated case, but not as much as the fill factor.

Tables III.6 : Table showing previous studie about Cu₂O /ZnO simulation results and our results

Parameter	Literature [42]	Our values
Voc (V)	1.093	1.87
Jsc (mA/cm²)	9.85	10.01
FF (%)	61.96	8.95
η (%)	6.67	1.68

Our results showed that when the Cu₂O layer thickness was increased from 0.5 μm to 2 μm, the cell efficiency improved from 1.28% to 1.68%. We also observed a slight improvement in open circuit voltage (Voc), short circuit current density (Jsc) and fill factor (FF) with increasing thickness within this range. To gain a broader perspective on the performance of Cu₂O solar cells, we compared our results tables III.5 and tables III.6 with those of another published study by researchers who also used the SCAPS-1D software. The results published by Abderrahim Sakkat et al. showed a much higher efficiency of 6.67% for a solar cell built on a 2 μm thickness Cu₂O layer. This remarkable difference in performance highlights the critical role of the overall device structure and composition, not just the thickness of the absorber layer. The incorporation of the ZnO layer is likely to contribute to improved charge extraction, reduced recombination or overall improved light absorption properties, leading to this significant increase in efficiency compared to our results which focused primarily on the effect of Cu₂O thickness in a simpler structure. We also note that both Voc and Jsc are higher than the reference values, while FF and efficiency are lower. We made another comparison of (Cu₂O) to other previous studies and the following table III.7 shows the values taken for them.

Table III.7: Summary of the Properties of the Materials included in the numerical simulation wok[41].

Material properties	p-Cu ₂ O	n-ZnO
Band gap(eV)	2.1	3.37
Electron Affinity(eV)	3.2	4.4
Dielectric Permittivity(relative)	7.6	9
Conduvtion Band Density of States (Cm⁻³)	2.2 x 10¹⁸	2.43 x 10¹⁹
Valence Band Density of States(Cm⁻³)	1.34x 10¹⁹	1.8x10¹⁹
Electron Thermal Velocity(cm/s)	1.0 x 10⁷	1.0 x 10⁷
Hole Thermal Velocity(cm/s)	1.0 x 10⁷	1.0 x 10⁷
Electron Mobility(cm²/Vs)	200	10
Hole Mobility(cm²/Vs)	100	5

The following table summarises the comparison between other studies results and our results.

Table III.8: Table showing someone's Cu₂O/ZnO simulation results and our results.

Parameter	Literature [41]	Our values
Voc (V)	0.77	1.87
Jsc (mA/cm²)	11.18	10.01
FF (%)	74.07	8.95
η (%)	6.36	1.68

Our results showed that the cell efficiency reached 1.68% at a Cu₂O layer thickness of 2 μm, with an open-circuit voltage (Voc) of 1.87 V, a short-circuit current density (Jsc) of 1.01 mA/cm² and a fill factor (FF) of 8.95%.

In contrast, other researchers achieved a 6.36% higher efficiency at a thickness of 70 μm, with a Voc of 0.77 V, a Jsc of 11.18 mA/cm² and an FF of 74.07%. It should be noted that our Voc value was better than other experimental values, while the Jsc, FF and efficiency values in the other experiments were higher. This is due to the different parameter values chosen for the simulation. The comparison was divergent in terms of thickness:

the thickness chosen in our experiment was 2 μm, much smaller than the 70 μm chosen in the comparison experiment. However, the cell efficiency values with open circuit voltage (Voc) were similar.

III.16. Conclusion

In summary, this chapter has provided the basic simulation framework using SCAPS-1D to evaluate the efficiency characteristics of Cu₂O and CuO thin film solar cells. Our initial parametric studies have highlighted the critical role of thickness and acceptor concentration in achieving optimal device performance.

device performance. In particular, our simulations indicate that the use of an absorber thickness of approximately 2 μm and maintaining an acceptor concentration (NA) greater than $1 \times 10^{16} \text{ cm}^{-3}$ are better choices for maximizing the simulated efficiency in both Cu₂O and CuO absorber-based solar cell configurations. The encouraging agreement between the simulated efficiency results under these conditions and the high conversion efficiencies documented in experimental studies for studies for Cu₂O and CuO solar cells provides strong validation for our simulation methodology. We will continue to explore the complex interplay of different device parameters, building on the identified importance of 2 μm absorber thickness and an NA greater than $1 \times 10^{16} \text{ cm}^{-3}$ to identify the most effective strategies for improving the conversion efficiency of these thin-

film photovoltaic technologies.

General Conclusion

General conclusion

In our work, we have investigated the electrical properties of CuO/ZnO and Cu₂O /ZnO heterojunction solar cells. Using the SCAPS-1D simulation tool, we have investigated CuO/ZnO and Cu₂O /ZnO heterojunction solar cell architectures under AM1.5G illumination at 300K. These designs include a highly doped n-type ZnO which acts as a window layer to minimize light reflection. The p-n junction is formed by the n-type ZnO window layer in conjunction with the p-type CuO and p-type Cu₂O absorber layers. By calculating the current-voltage (I-V) characteristics for various thin-film thin film parameter adjustments, we were able to determine key photovoltaic performance metrics, including short-circuit current density (JSC), open-circuit voltage (VOC) voltage (VOC), fill factor (FF), and photovoltaic conversion efficiency (η).

The behavior of these solar cells was studied and analyzed by varying several physical and geometrical physical and geometrical parameters, especially the thickness of the p-CuO and p-Cu₂O absorber layers, as well as the Cu₂O absorber layers and the acceptor concentrations NA (CuO) and NA (Cu₂O).

Our results indicate that changing the geometric properties of the solar cell structures based on p-CuO and p-Cu₂O absorbers, specifically the thickness of the CuO and Cu₂O absorber layers, has a much more effect on the electrical cell electrical properties than changes in the properties of the ZnO window layer. The optimal thickness for both absorber layers was found to be 2 μm . It's clear that the electrical performance of solar cells using CuO and Cu₂O as light is significantly influenced by their intrinsic physical properties, especially the acceptor concentration (NA). Our simulations indicate that to achieve the most effective performance requires that this acceptor concentration be kept within a range, identified as 10^{16} cm^{-3} to 10^{18} cm^{-3} . The results generated by the SCAPS simulation tool show a level of accuracy and consistency that compares favorably with previously studies's results.

References

- [1] V. Fthenakis, "Sustainability of photovoltaics: The case for thin-film solar cells," *Renew. Sustain. Energy Rev.*, vol. 13, no. 9, pp. 2746–2750, 2009, doi: 10.1016/j.rser.2009.05.001.
- [2] D. B. Mitzi, O. Gunawan, T. K. Todorov, K. Wang, and S. Guha, "The path towards a high-performance solution-processed kesterite solar cell," *Sol. Energy Mater. Sol. Cells*, vol. 95, no. 6, pp. 1421–1436, 2011, doi: 10.1016/j.solmat.2010.11.028.
- [3] N. Naghavi *et al.*, "Ultrathin Cu(In, Ga)Se₂ solar cells," in *Conference Record of the IEEE Photovoltaic Specialists Conference*, 2011, pp. 003642–003645. doi: 10.1109/PVSC.2011.6185938.
- [4] V. M. Fthenakis, "End-of-life management and recycling of PV modules," *Energy Policy*, vol. 28, no. 14, pp. 1051–1058, 2000, doi: 10.1016/S0301-4215(00)00091-4.
- [5] M. Abdelfatah, N. M. El-Shafai, W. Ismail, I. M. El-Mehasseb, and A. El-Shaer, "Simulation of CuO/ZnO heterojunction for photovoltaic applications," *IOP Conf. Ser. Mater. Sci. Eng.*, vol. 956, no. 1, p. 012005, Oct. 2020, doi: 10.1088/1757-899X/956/1/012005.
- [6] K. Ungeheuer *et al.*, "Influence of Cr Ion Implantation on Physical Properties of CuO Thin Films," *Int. J. Mol. Sci.*, vol. 23, no. 9, 2022, doi: 10.3390/ijms23094541.
- [7] "Copper Oxide: Learn Definition, Formula, Structure & Properties." Accessed: Feb. 17, 2025. [Online]. Available: <https://testbook.com/chemistry/copper-oxide>
- [8] K. Nakamura, M. Tanabe, S. Abe, T. Mawatari, and T. Nakagaki, "Modeling of low-temperature reduction of metal oxide in hydrogen treatment system for severe accidents in nuclear power plants," *Int. Conf. Nucl. Eng. Proceedings, ICON*, vol. 3, 2020, doi: 10.1299/mej.21-00005.
- [9] Cuprous oxide (CHEBI:81908). Accessed: Feb. 17, 2025 [Online]. Available: <https://www.ebi.ac.uk/chebi/searchId.do?chebiId=CHEBI:81908>
- [10] A. A. Aref, L. Xiong, N. Yan, A. M. Abdulkarem, and Y. Yu, "Cu₂O nanorod thin films prepared by CBD method with CTAB: Substrate effect, deposition mechanism and photoelectrochemical properties," *Mater. Chem. Phys.*, vol. 127, no. 3, pp. 433–439, 2011, doi: 10.1016/j.matchemphys.2011.02.029.
- [11] Coleman, Victoria A., and Ch Jagadish. "Basic properties and applications of ZnO." *Zinc oxide bulk, thin films and nanostructures*. Elsevier Science Ltd, 2006. 1-20.
- [12] Zinc Oxide (ZnO) Semiconductors. Accessed: Mar. 04, 2025 [Online]. Available: <https://www.azom.com/article.aspx?ArticleID=8417>
- [13] S. Bognár, P. Putnik, and D. Š. Merkulov, "Sustainable Green Nanotechnologies for Innovative Purifications of Water: Synthesis of the Nanoparticles from Renewable Sources," *Nanomaterials*, vol. 12, no. 2, 2022, doi: 10.3390/nano12020263.
- [14] Schubert, E. F. (2015). Doping in III-V semiconductors. E. Fred Schubert..
- [15] "Copper(II)_oxide." Accessed: Mar. 04, 2025. [Online]. Available: https://www.chemeurope.com/en/encyclopedia/Copper%28II%29_oxide.html
- [16] Patwary, Md Abdul Majed, et al. "Copper oxide nanostructured thin films processed by SILAR for optoelectronic applications." *RSC advances* 12.51 (2022): 32853-32884.
- [17] W. H. Brattain, "The copper oxide rectifier," *Rev. Mod. Phys.*, vol. 23, no. 3, pp. 203–212, 1951, doi: 10.1103/RevModPhys.23.203.
- [18] M. Dahrul, H. Alatas, and Irzaman, "Preparation and Optical Properties Study of CuO thin Film as Applied Solar Cell on LAPAN-IPB Satellite," *Procedia Environ. Sci.*, vol. 33, pp. 661–667, 2016, doi: 10.1016/j.proenv.2016.03.121.
- [19] C. H. Lee, C. S. Ritz, M. Huang, M. W. Ziwocky, R. J. Blise, and M. G. Lagally, "Integrated freestanding single-crystal silicon nanowires: Conductivity and surface treatment," *Nanotechnology*, vol. 22, no. 5, 2011, doi: 10.1088/0957-4484/22/5/055704.
- [20] Sun, Shaodong, et al. "Cuprous oxide (Cu₂O) crystals with tailored architectures: A comprehensive review on synthesis, fundamental properties, functional modifications and applications." *Progress in Materials Science* 96 (2018): 111-173. [21] D. Aldakov, "J Materials Chemistry C," *J. Mater. Chem.*, vol. 1, no. 207890, p. 3777, 2020, [Online]. Available: <http://ncsr.unl.edu/wordpress/wp-content/uploads/2010/07/Synthesis-of-high-quality-inverse-opals-J-Mater-Chem-C-article.pdf>
- [22] "What is Cuprite – Geology In." Accessed: Mar. 04, 2025. [Online]. Available: https://www.geologyin.com/2014/05/cuprite.html?utm_source=chatgpt.com
- [23] L. M. Mahlaule-Glory and N. C. Hintsho-Mbita, "Green Derived Zinc Oxide (ZnO) for the Degradation of Dyes from Wastewater and Their Antimicrobial Activity: A Review," *Catalysts*, vol.

12, no. 8, 2022, doi: 10.3390/catal12080833.

- [24] J. K. Jogi, S. K. Singhal, A. Tanna, M. Singh, and P. Mishra, "Synthesis of ZnO nanostructures and their medical applications," *Oxides Med. Appl.*, pp. 147–165, Jan. 2023, doi: 10.1016/B978-0-323-90538-1.00012-1.
- [25] C. Romano, T. Lam, G. A. Newsome, J. A. Taillon, N. Little, and J. sun Tsang, "Characterization of Zinc Carboxylates in an Oil Paint Test Panel," *Stud. Conserv. = Etudes Conserv.*, vol. 65, no. 1, p. 10.1080/00393630.2019.1666467, Jan. 2020, doi: 10.1080/00393630.2019.1666467.
- [26] K. L. Dionisio *et al.*, "Data Descriptor: The Chemical and Products Database, a resource for exposure-relevant data on chemicals in consumer products," *Sci. Data*, vol. 5, Jul. 2018, doi: 10.1038/SDATA.2018.125.
- [27] X. W. Sun, Z. J. Liu, Q. F. Chen, H. W. Lu, T. Song, and C. W. Wang, "Heat capacity of ZnO with cubic structure at high temperatures," *Solid State Commun.*, vol. 140, no. 5, pp. 219–224, 2006, doi: 10.1016/j.ssc.2006.08.024.
- [28] prof. Dr. ir. Marc Burgelman, Dr. ir. Koen Decock, Dr. ir. Johan Verschraegen, Dr. ir. Alex Niemegeers, and ir. Stefaan Degrave, "Simulation programme SCAPS-1D for thin film solar cells developed at ELIS, University of Gent," University of Gent, Dept. Electronics and Information Systems (ELIS) Pietersnieuwstraat 41 B-9000 Gent, Belgium. Accessed: Jun. 14, 2025. [Online]. Available: <https://scaps.elis.ugent.be/>
- [29] M. Burgelman, K. Decock, A. Niemegeers, J. Verschraegen, and S. Degrave, "SCAPS manual".
- [30] C. Series, "Numerical analysis and optimization of Cu₂O/TiO₂, CuO / TiO₂, heterojunction solar cells using SCAPS Numerical analysis and optimization of Cu₂O/TiO₂, CuO / TiO₂, heterojunction solar cells using SCAPS," 2018.
- [31] E. Technologies, "Development of Metal Oxide Solar Cells through Numerical Modelling Le Zhu," 2012.
- [32] T. K. S. Wong, S. Zhuk, S. Masudy-Panah, and G. K. Dalapati, "Current status and future prospects of copper oxide heterojunction solar cells," *Materials (Basel)*, vol. 9, no. 4, pp. 1–21, 2016, doi: 10.3390/ma9040271.
- [33] L. Boudaoud, S. Khelifi, M. Mostefaoui, A. K. Rouabhia, and N. Sahouane, "Numerical Study of InGaN based Photovoltaic by SCAPS Simulation," *Energy Procedia*, vol. 74, pp. 745–751, 2015, doi: 10.1016/j.egypro.2015.07.810.
- [34] O. Access, "Simulation and Optimization of ZnO/CuO/Cds Solar Cell Using SCAPS," pp. 97–100, 2023.
- [35] S. N. Puspita and Y. S. Permana, "Tinjauan Yuridis Ketentuan Upah Pekerja / Buruh Berdasarkan Undang Undang Cipta Kerja Pasca Putusan Mahkamah Konstitusi Nomor," vol. 03, no. 01, pp. 78–83, 2025..
- [36] N. D. Lam, "Modelling and numerical analysis of ZnO / CuO / Cu₂O heterojunction solar cell using SCAPS Modelling and numerical analysis of ZnO / CuO / Cu₂O heterojunction solar cell using SCAPS," 2020.
- [37] P. Sawicka-Chudy, M. Sibiński, E. Rybak-Wilusz, M. Cholewa, G. Wiesz, and R. Yavorskyi, "Review of the development of copper oxides with titanium dioxide thin-film solar cells," *AIP Adv.*, vol. 10, no. 1, 2020, doi: 10.1063/1.5125433.
- [38] P. Jiang and H.-Z. Zheng, *The Physics of Semiconductors*. 1993. doi: 10.1142/9789814536738.
- [39] M. Abdelfatah, N. M. El-Shafai, W. Ismail, I. M. El-Mehasseb, and A. El-Shaer, "Simulation of CuO/ZnO heterojunction for photovoltaic applications," *IOP Conf. Ser. Mater. Sci. Eng.*, vol. 956, no. 1, 2020, doi: 10.1088/1757-899X/956/1/012005.
- [40] A. Sekkat, D. Bellet, G. Chichignoud, D. Muñoz-Rojas, and A. Kaminski-Cachopo, "Unveiling Key Limitations of ZnO/Cu₂O All-Oxide Solar Cells through Numerical Simulations," *ACS Appl. Energy Mater.*, vol. 5, no. 5, pp. 5423–5433, 2022, doi: 10.1021/acsaem.1c03939.
- [41] K. Naceur, "Simulation of cuprous oxide solar cells using SILVACO TCAD," *Opt.-Int.J.Light Electron Opt.*, vol. 127, Issue, 2023, [Online]. Available: [http://thesis.univ-biskra.dz/6196/1/Final thesis khadidja naceur.pdf](http://thesis.univ-biskra.dz/6196/1/Final%20thesis%20khadidja%20naceur.pdf)